UNITED NATIONS EDUCATIONAL, SCIENTIFIC AND CULTURAL ORGANIZATION
INTERNATIONAL ATOMIC ENERGY AGENCY
INTERNATIONAL CENTRE FOR THEORETICAL PHYSICS
I.C.T.P., P.O. BOX 586, 34100 TRIESTE, ITALY, CABLE: CENTRATOM TRIESTE

H4.SMR/1058-7

WINTER COLLEGE ON OPTICS

9 - 27 February 1998

Near Field Optical Microscopy

D. Van Labeke

Laboratoire P.M. Duffieux, Université de Besançon, France

AN INTRODUCTION TO SCANNING NEAR-FIELD OPTICAL MICROSCOPY

Daniel VAN LABEKE
Laboratoire P.M. Duffieux
Université de Besançon, CNRS UMR 6603
UFR Sciences et Techniques
route de Gray, 25030 Besançon Cedex
Tel: 33.3.81.66.64.14, Fax: 33.3.81.66.64.14
Email:daniel.vanlabeke@univ-fcomte.fr

January 1998

Abstract

Lectures given during the Winter School on Optics
Trieste 9-27 February 1998

This paper is only an introduction to near-field optics and to near-field microscopy. After an historical introduction, we describe the various current configurations and present the technical problems and their solutions. Then, the theoretical principle of near-field microscopy is exposed, we explain how by using evanescent waves the Abbe-Rayleigh diffraction limit can be bypassed. Two simple pedagogical models of near-field optical microscopes are presented. The results in resolution and many applications are described. The last chapter is devoted to a comparison and a rapid description of more rigorous theoretical methods.

Contents

1 Introduction 4

2 Far-field Microscopy and Local Probe Microscopy 5
- 2.1 Far-field Microscopy . . . 5
- 2.2 Local Probe Microscopy . . . 7

3 History of Near-field Microscopy 8

4 Various configurations of SNOM 9

5 Theoretical principle of near-field microscopy 12
- 5.1 Dispersion equation . . . 12
- 5.2 Evanescent waves in vacuum . . . 13
- 5.3 Transversal resolution of an optical microscope . . . 15

6 Optical Tunneling 16
- 6.1 Fresnel's evanescent wave . . . 16
- 6.2 Optical Tunneling . . . 17

7 Near-Field and Far-field: two examples 18
- 7.1 Radiating dipole . . . 18
- 7.2 Diffraction theory . . . 20

8 Diffraction and evanescent waves. Plane Wave Expansion 21
- 8.1 Plane Wave Expansion[98, 83] . . . 21
- 8.2 Influence of propagation on the Plane Wave Expansion of the field . . . 23
- 8.3 Far-field and near-field microscopy . . . 24
- 8.4 Tip-sample distance and resolution . . . 25
- 8.5 Relation between Plane Wave Expansion and usual diffraction theories . . . 26
- 8.6 Asymptotic limit of a Plane Wave Expansion . . . 27

9 Simple models of Scanning Near-Field Microscopes 27
- 9.1 A simple model of STOM . . . 27
  - 9.1.1 The model . . . 27
  - 9.1.2 Calculation of the detected intensity . . . 28
- 9.2 A simple model of SNOM . . . 30
  - 9.2.1 The model . . . 30
  - 9.2.2 The nano-source field . . . 30
  - 9.2.3 Calculation of the detected intensity . . . 31
  - 9.2.4 Discussion . . . 32

10 Technical problems and their solutions 33
- 10.1 Scanning . . . 33
- 10.2 Vibration isolation . . . 33
- 10.3 Light sources . . . 34
- 10.4 Detection . . . 34
- 10.5 Control of tip position . . . 34
- 10.6 Probe fabrication . . . 35
  - 10.6.1 Tapered optical fiber . . . 35
  - 10.6.2 Other tips . . . 36
  - 10.6.3 Alternative probes . . . 37

11 Results and Applications 37
- 11.1 Resolution limits . . . 37
- 11.2 Spectroscopies . . . 38
- 11.3 Local studies of optical components . . . 39
- 11.4 Magneto-optical materials and mass storage . . . 40
- 11.5 Photolithography . . . 40
- 11.6 Biology . . . 41

12 Theoretical methods 41
- 12.1 Classifications of theoretical schemes . . . 42
  - 12.1.1 Microscopic or macroscopic theory . . . 42
  - 12.1.2 Global or non-global theory . . . 43
- 12.2 Coupled dipoles and multipoles methods . . . 43
- 12.3 The multiple multipole method (MMP) . . . 43
- 12.4 Volume integral method . . . 44
- 12.5 Macroscopic surface integral method . . . 44
- 12.6 First order perturbation method . . . 45

13 Conclusion 46

14 Acknowledgements 47

1 Introduction

Near-field optical microscopy is a new technique to image and study a sample with light and with a sub-micron lateral resolution. The idea is old, it was proposed 70 years ago in a prophetical paper by E.H Synge [99], but the real development only began in the early eighties. In 1984 D. Pohl [92] reached a resolution of $\lambda/20$ (30 nm). The first true applications were presented in 1993 [10]. An image with a nanometric resolution is published in 1995 [104] . Today, the pioneer works are achieved and many papers are published that propose many applications in a large variety of domains.

This paper is just an introduction to near-field optical microscopy. It is found on my lectures given in Besançon for PhD students and it only gives the main faitures of this new area of optics.

Many papers are now available and it is no longer possible to give a complete bibliography. Two books are published:

"Near-field Optics and nanoscopy" by J.P. Fillard (Word Scientific 1996)

"Near-Field Optics" by M.A. Paesler and P.J. Moyer (J. Wiley and Sons, 1996)

Many references can be found in the proceedings of the international conference on Near-field Optics:

- **"Near-Field Optics I "**: Besançon 1992

Edited by D. Pohl and D. Courjon, Nato Series E vol 242 (Kluver Academic, 1993).

- **"Photon and local probes"** Konttanz 1994

Edited by O. Marti and R. Möller Nato Series E vol 300 (Kluver Academic, 1995).

-**"Near-field Optics II"**, Raleigh 1993, Ultramicroscopy volume 57, Nos. 2-3, pp113-322 (1995).

-**"Near-field Optics III"**, Brno 1995, Ultramicroscopy, volume 61 Nos.1-4, pp 1-311 (1995)

-**Near-field Optics IV**, Jerusalem 1997, to be published in Ultramicroscy.

-**"Near-Field Optics V"**, Tokyo 1998.

It is also possible to begin with review papers:

-**"Scanning near-field optical microscopy"** D.W. Pohl Advances in optical and electron Microscopy 12 (1991)

-**"Near-field microscopy and near-field optics"** D. Courjon and C. Bainier, Physics Report 57, pp 989-1028 (1994)

-**"Theoretical problems in scanning near-field optical microscopy"** D. Van Labeke, Near-Field Optics I pp 157-178 (1993)

-**"Near-field optics theory"**, C. Girard and A. Dereux, Rep. Prog. Phys. 59 pp657-699 (1996).

2 Far-field Microscopy and Local Probe Microscopy

In 1981, Binning and Rohrer designed and built the first Scanning Tunneling electronic Microscope (STM). Their invention is the beginning of a new development in microscopy and has rapidly led to many kinds of new microscopes. They are at the origin of a new microscopy that is called: Near Field Microscopy or Local Probe Microscopy.

2.1 Far-field Microscopy

In a conventional microscope the most important part is a lens, the objective lens. The sample is illuminated by transmission or reflection and the objective collects the light emitted by the sample. The objective is far-from the sample, at a few mm, so at many wavelengths. So the name of this kind of microscope is Far Field Microscope (Fig.1)

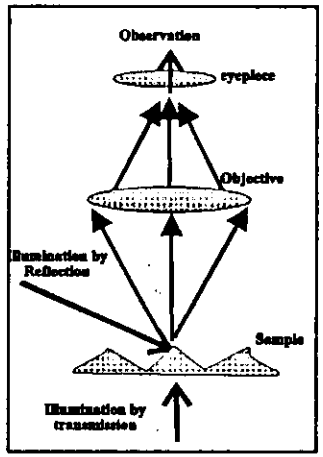

Figure 1: Principle of a Far-field microscope

In the following, the z direction will be perpendicular to the mean plane of the sample that is the (x, y) plane.

A microscope is an apparatus for imaging small details and its quality will be defined by its resolution power. But two resolutions have to be distinguished. In the z direction, it seems to have no limit to the resolution. By interferometry or ellipsometry, a microscope can measure thickness variations as small as $10^{-3}nm$. On the contrary, the transversal resolution, in the (x-y) plane is theoretically limited. Light is a wave and even for a perfect objective, without aberrations, the image of a point is not a point but a diffraction spot. Diffraction of light by the objective limits the resolving power of the microscope. At the end of the XIX^{th} century Abbe-Rayleigh have demonstrated a criterion which implies that two points, A, B, of the sample cannot be separated if their distance is smaller than a minimum. For incoherent illumination and a spherical objective lens, the Abbe-Rayleigh criterion has for expression:

$$AB \geq \delta = \frac{0.6\lambda}{n\sin(\theta_A)} \tag{1}$$

In this equation λ is the wavelength of the light, n is the optical index of the medium between sample and the objective. Usually, this medium is air, but to decrease δ and to increase the resolution it can be useful to put a drop of a liquid of high index between the sample and the objective. The angle θ_A measures the aperture of the microscope. When θ_A is increased, the luminosity and the resolution of the microscope is increased. $n\sin(\theta_A)$ is thus a very important parameter of a conventional microscope and is called the Numerical Aperture (NA):

$$NA = n\sin(\theta_A) \tag{2}$$

But when θ_A is large, the objective does not work in the Gauss approximation and the aberrations must be corrected. So a microscope objective with a large NA is composed of many lenses and is very expensive.

With visible light ($0.4\mu m \leqslant \lambda \leqslant 0.8\mu m$) and a very good objective (NA=1.2) the smallest theoretical value of δ is around $\lambda/2 \approx 0.25\mu m$. But, because the aberrations of the lenses are not completely corrected the practical resolution limit is around 0.5 μm and often larger than 1 μm.

A solution to decrease δ is to use electromagnetic radiation with shorter wavelength. In the Ultraviolet region only quartz can be used to build lenses and the aberrations cannot be corrected. To have good images, the NA aperture must be very small. Consequently, till now, Ultraviolet conventional microscope has a lesser resolution than a visible one.

Conventional electronic microscopes (TEM: Transmission Electronic Microscope and SEM: Scanning Electronic Microscope) are also a far-field microscope. Their principle are the same than the optical microscope, but light is replaced by electrons and glass lenses are replaced by magnetic ones.

2.2 Local Probe Microscopy

For a local probe microscope (Fig.2) the image is not obtained by using an objective lens. The most important part is a very small probe (generally a tip) that is scanned at a very small distance from the sample. These microscopes are scanning microscopes, the image is obtained by moving the probe point after point and then by plotting the detected signal versus probe position. A local probe microscope needs a computer to draw the images but also to control probe displacement and positions. By changing the nature of the probe the microscope will be sensible to another physical phenomenon and so various kinds of local probe microscope can be constructed.

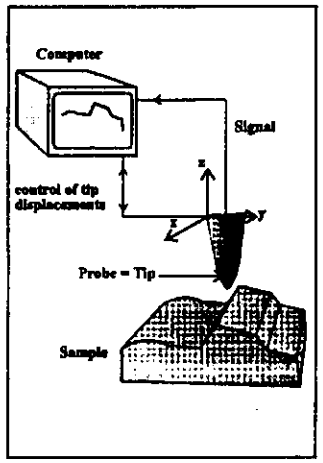

Figure 2: Principle of a Scanning Probe Microscope

In the STM, there is an electronic tunneling current between the tip and the sample and the detected signal is an electric current. If we measure the force between tip and sample, we obtain a Scanning Force Microscope (SFM) that is also called an Atomic Force Microscope (AFM). If the probe is used

for illuminating the sample of for collecting light above the sample we obtain a Scanning Near-field Optical Microscope (SNOM). The three previous local probe microscopes are the most important ones, but there are many others local probe microscopes: magnetic force microscope, electrostatic force microscope, Kelvin probe microscope, thermal probe microscope...

Local probe Microscopes have a resolving power that is not limited by diffraction, and lead to images with a resolution unexpected few years ago. STM has reached the atomic resolution and AFM the molecular one. Commercial STM and AFM are sold with a warranted subnanometric lateral resolution. SNOM is still in development and it has not yet reached such a high lateral resolution. But many laboratories produce in routine images with a lateral resolution around 20 nm and one group has reached the nanometer scale.

3 History of Near-field Microscopy

In fact, local probe microscopy was invented 50 years before Binning and Rohrer. The principle of Scanning Optical Near-field Microscopy was fully described in a prophetical paper by E.H. Synge [99]. In that paper, the author suggested a method to increase the resolution of optical microscope: using a nano-aperture in a thin metallic screen to scan the near-field at a few nanometers above a sample. In a letter to Einstein, he also suggested to utilize a metallized quartz tip as a probe, that is a solution that is used at the present day.

However this paper was forgotten and the first experiments only began in 1972. For obvious technical reasons they were firstly carried out in radiowaves [1] and in Infrared [80]. The first experiments in the optical domain started after the invention of the STM. Moreover, the first Scanning Optical Near-field microscope was built in 1983 by D. Pohl [91] in the laboratory of Binning and Rohrer. Other prototypes were carried out few months later at Cornwell university [72].

Those preliminary experiments used for the probe the configuration suggested fifty years ago by Synge: a small aperture in a metallic screen. But that solution is not very convenient because it is impossible to move a metallic screen at a few nanometers of a sample without collisions. The true development of scanning near-field optical microscopy occurred when experimentalists decided to employ a tip as an optical probe. In 1984 a tapered quartz is obtained by chemical etching of a quartz crystal [92]. The American group used for the same purpose a micro-pipette that was tapered by heating [15].

In the first experiments the tip was used as a nano-source for illuminating

the sample. The first microscope where the tip is used to collect the sample near-field was built in 1987 [14], in 1988 was published the first results obtained by a SNOM working in reflection [34]. In 1989 3 groups proposed a new configuration [94, 24, 27] which is a true tunneling optical microscope, the analog in the optical domain of the STM. This near-field microscope is thus called Scanning Tunneling Optical Microscope (STOM) or Photon Scanning Tunneling Microscope (PSTM).

4 Various configurations of SNOM

After those pioneer works many apparatus have been built and have obtained images. In this chapter we just present the principle of the configurations that are today the most frequently employed and that lead to best results.

In order to classify the configurations we propose two criteria. Firstly, as in conventional microscopy, we have to distinguish **transmission or reflection microscopes**. But a criterion specific to near-field microscopes is to check how the probe is operated. There are 3 different modes of using the probe: the **illumination mode**, the **collection mode** and the **perturbation mode.**

In the **illumination mode** the probe acts as a nano-source for illuminating the probe at a small distance. The diffracted light is thus far-field collected.

In the **collection mode** the sample is illuminated by a far-field conventional source and the probe is used for collecting the near-field above the sample.

In the **perturbation mode**, the probe is used neither for illuminating, nor for collecting light. It seems to be optically passive. But, being immersed in the sample near-field, it modifies the boundary conditions, which implies modifications of the optical signal.

Today most of the near-field microscopes used a tapered tip as a probe. Four kinds of transmission SNOM are plotted in (Fig.3). In (Figs.3a), the tip is used in the emission mode and the diffracted light is far-field collected by a lens. In (Fig. 3b), the sample is far-field illuminated through a lens and the diffracted light of the sample is collected by the tip in the near-field region. Apparatus of (Figs.3a and 3b) are the same, the second one can be obtained from the first one by simply inverting the direction of light propagation. In the two previous set-up the lens has no function in the image formation, it is only used for light collection or concentration.

The principle of the Scanning Tunneling Optical Microscope (STOM) is presented in (Fig.3c). The sample is at the surface of a glass lens (hemi-

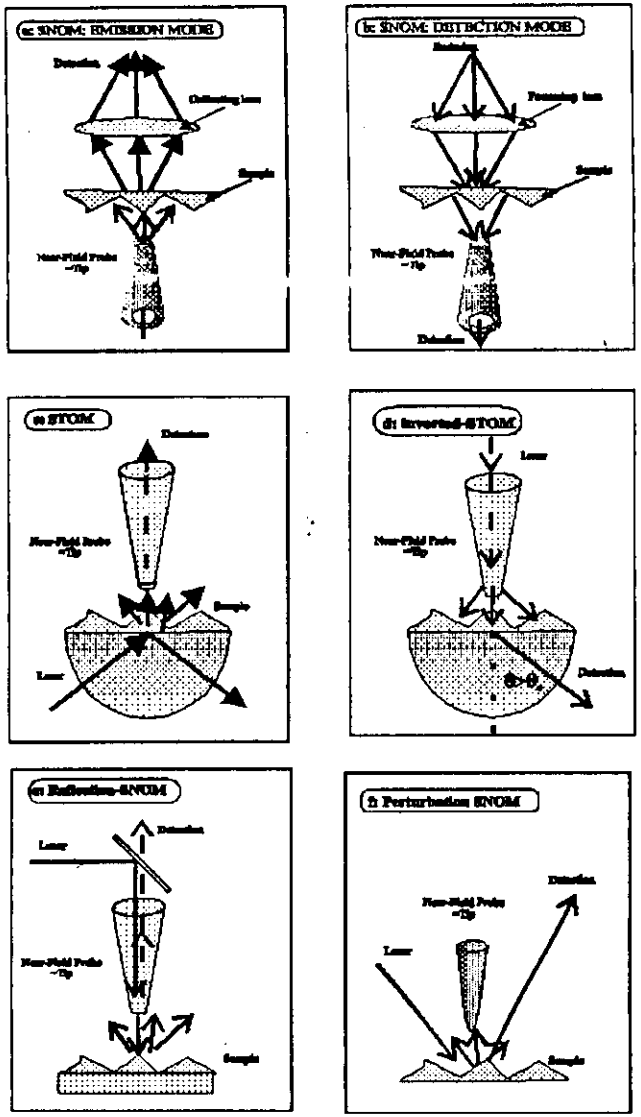

Figure 3: Different configurations of Scanning Optical Near-Field Microscope

spherical or cylindrical) and it is illuminated through the glass by a light beam. The angle of incidence is above the critical angle, so the sample is illuminated in total internal reflection by an evanescent wave.

Recently, D. Pohl [52] proposed a very ingenious configuration (Fig.3d). The sample is on the plane face of a hemispherical lens, the tip is used in the emission mode, diffracted light is far-field collected, but the direction of detection can be changed. When detection is performed in normal direction the apparatus is a SNOM like (Fig.3a). When light is detected in the "forbidden region", that corresponds to an angle of detection above the critical one, the detected signal is mediated through evanescent waves and the apparatus is working by optical tunneling and can be called an inverted STOM (I-STOM [71]).

The previous apparatus are transmission microscopes and their samples must be transparent. However it will be necessary for many applications to study in near-field non-transparent samples: metals, semiconductors... For this purpose M. Spajer [96] designed and built a near-field microscope where the tip is used both for illumination and detection (Fig.3e). The tip is the tapered end part of an optical fiber, the light travels through the tip for illuminating the sample and then the detected light travels back in the opposite direction. In the following this microscope will be called a Reflection SNOM (R-SNOM).

In the first experiments SNOM (Figs. 3a-b) utilized a probe which was a metallized tapered optical fiber except the end part of the apex (small aperture tip). On the contrary the first experiments of STOM and R-SNOM (Figs. 3c-e) were performed with a tapered optical fiber without any metallization (dielectric tip). Today the two kinds of tips are used on every configuration.

SNOM and STOM have demonstrated that they can provide images with a lateral resolution far below the Abbe-Rayleigh criterion. It is difficult to exactly precise the resolution limit, it depends on the sample and mainly it depends on the precise definition of the resolution that is used. We can consider that it is better than 30 nm. [4] and that 15 nm can be reached [17].

For technical reasons the lateral resolution of the R-SNOM is worse. The light has to travel twice the tip and the detected signal is very small, and it is difficult to separate signal and noise. The resolution seems to be around 100 nm for the R-SNOM.

Recently, the development of SNOM working in the perturbation mode has led to a very important improvement of the resolution. The principle of this new mode can be found in an American patent by Wickramasinghe and Williams in 1990 [103] : it consists to use a tip to pertub the near-field, the modifications being far-field detected. In 1992 Specht et al used a STM tip

to modify a surface plasmon resonance [97]. This modification is measured in far-field by studying the reflected intensity versus tip position. The group of A.C. Boccara [2] in Paris, France, has built a near-field microscope working in reflection where a metallic tip is immersed in the light spot on the sample and by far-field detecting the induced diffracted field (Fig. 3f). The first results of Wickramasynghe et al were published in 1995. They used a very sensitive interferometric method to detect the optical perturbation due to the tip and thus they are able to produce images showing 1 nm details without ambiguity [104].

5 Theoretical principle of near-field microscopy

The Abbe-Rayleigh limit is a theoretical limit and it is generally supposed that it cannot be bypassed. Moreover in many textbooks this diffraction limit is generally demonstrated by using the Heisenberg's relations that enhance the sacred character of the resolution limit. In this chapter we will describe the theoretical principle of near-field microscopy and theoretically explain how, by using evanescent waves, the Abbe-Rayleigh limit can be bypassed while the Heisenberg's relations remain valid.

5.1 Dispersion equation

Light is an electromagnetic wave that verifies Maxwell equations. In the following we only consider monochromatic waves, we use complex notations (i=$\sqrt{-1}$)and we note c the speed of light in vacuum and $\lambda = \frac{2\pi}{\omega}$ the wave length in vacuum. We consider a plane wave propagating in a medium of dielectric constant ϵ and optical index n ($\epsilon = n^2$):

$$\vec{E}(x,y,z) = \vec{E}(\vec{r}) = \vec{E}_0 e^{i\vec{k}.\vec{r}-i\omega t} \tag{3}$$

Far from any sources, charge and current are equal to zero, consequently Maxwell equations imply that the Electric field verify the Helmoltz equation:

$$\Delta\vec{E}(x,y,z) + \epsilon\frac{\omega^2}{c^2}\vec{E}(x,y,z) = 0 \tag{4}$$

Thus, the wave vector $\vec{k}$ verifies the dispersion equation:

$$\vec{k}.\vec{k} = \left(\vec{k}\right)^2 = \epsilon\frac{\omega^2}{c^2} = \frac{n^2\omega^2}{c^2} \tag{5}$$

An homogeneous plane wave has a real $\vec{k}$ vector. If there is absorption in the medium, the dielectric constant is complex, the wave vector is also complex and the plane wave is an attenuated, inhomogeneous wave.

Let us notice that, even with a complex $\vec{k}$ vector, it is not the square modulus of $\vec{k}$ that occurs in the dispersion equation but the scalar product of $\vec{k}$ by itself.

5.2 Evanescent waves in vacuum

Let us consider now a plane wave propagating in vacuum. An homogeneous plane wave has a real wave vector. In this case the length of $\vec{k}$ is $k = \sqrt{\left(\vec{k}\right)^2} = \frac{\omega}{c}$ and each component has a length smaller than the length of the vector. For instance:

$$\boxed{k_x \leq \frac{\omega}{c} = \frac{2\pi}{\lambda} \qquad \text{when } \vec{k} \text{ is real}} \tag{6}$$

But, in vacuum, we can also consider the propagation of an attenuated plane wave with a complex wave vector. In this case, we note $\vec{k'}$ and $\vec{k''}$ respectively the real part and the imaginary part of $\vec{k}$:

$$\vec{k} = \vec{k'} + i\,\vec{k''} \tag{7}$$

We can thus simply separate the real part and the imaginary part of the dispersion equation (5):

$$\vec{k}.\vec{k} = \vec{k'}.\vec{k'} - \vec{k''}.\vec{k''} + 2i\,\vec{k'}.\vec{k''} = \frac{\omega^2}{c^2} \Longrightarrow \begin{cases} \vec{k'}.\vec{k'} - \vec{k'}.\vec{k''} = \frac{\omega^2}{c^2} \\ \vec{k'}.\vec{k''} = 0 \end{cases} \tag{8}$$

The second equation implies that the two real vectors, $\vec{k'}$ and $\vec{k''}$, are perpendicular. In vacuum, an attenuated plane wave with a complex wave vector, corresponds to a plane wave propagating without attenuation along $\vec{k'}$, but exponentially attenuated along a perpendicular direction:

$$\vec{E}(x,y,z) = \vec{E}(\vec{r}) = \vec{E}_0 \exp\left[-\vec{k''}.\vec{r}\right] \exp\left[i\left(\vec{k'}.\vec{r} - \omega t\right)\right] \tag{9}$$

For such a "disassociated" wave the equi-amplitude planes are perpendicular to the equi-phase ones. This kind of wave is called an **evanescent wave.**

Without restriction, the x-axis can be taken along $\overrightarrow{k'}$ and the z-axis along $\overrightarrow{k''}$. The first equation in (8) implies the x componant of the wavevector of the evanescent wave is greater than $\frac{2\pi}{\lambda}$:

$$k_x = \sqrt{\frac{\omega^2}{c^2} - (k_z)^2} = \sqrt{\left(\frac{2\pi}{\lambda}\right)^2 + (k'')^2} \geq \frac{2\pi}{\lambda} \qquad \text{For an evanescent wave} \tag{10}$$

Moreover, the decay length of the evanescent wave is proportional to the inverse of imaginary part of the wave vector: $L = 1/k''$. So, **more rapidly the evanescent wave is attenuated along the z axis, longer is the transversal component of the wave vector.**

It is also interesting to consider the energy flow associated with an evanescent wave. The time averaged value of the Poynting vector has for expression:

$$\left\langle \overrightarrow{P} \right\rangle = \frac{1}{4\mu_0}\left(\overrightarrow{E} \Lambda \overrightarrow{B^*} + \overrightarrow{E^*} \Lambda \overrightarrow{B}\right) \tag{11}$$

For a plane wave with a complex wave vector, the time averaged Poynting vector has thus for expression:

$$\left\langle \overrightarrow{P} \right\rangle = \frac{\exp\left[-2\overrightarrow{k''}.\overrightarrow{r}\right]}{2\omega\mu_0}\left[\overrightarrow{k'}\left|\overrightarrow{E_0}\right|^2 + \overrightarrow{k''} \Lambda \left(\mathrm{Re}(\overrightarrow{E_0}) \Lambda \mathrm{Im}(\overrightarrow{E_0})\right)\right] \tag{12}$$

If the plane wave is homogeneous, the wave vector is real and the energy flow is parallel to $\overrightarrow{k} = \overrightarrow{k'}$ and proportional to the square modulus of the field amplitude.

The second term equation (12) is unusual. It does not vanish only if the wave vector is complex and if the wave is elliptically (or circularly) polarized. This term leads to an **energy flow that is not parallel to the wave vector** and it closely related to the transversal shift obtained for total internal reflection[55, 56].

However, for any polarization and any wave vector we have always: $\left\langle \overrightarrow{P} \right\rangle . \overrightarrow{k''} = 0$ and consequently, **for an evanescent wave the energy flow is always in a plane perpendicular to $\overrightarrow{k''}$** . It is parallel to $\overrightarrow{k'}$ if the plane is linearly polarized.

5.3 Transversal resolution of an optical microscope

We consider an illuminated object in the x-y plane. It creates an electric field with a width δx in real space. The detected light corresponds to a distribution of wave vectors with a width δk_x in the reciprocal space. A general property of Fourier transform connects the two widths:

$$\delta x \delta k_x \geq 2\pi \tag{13}$$

The precise value of the numerical factor in (13) depends on the definition of the width (root mean squared, half height width...).

In a conventional microscope, the objective lens is far-from the sample and only homogeneous waves can be collected. The angular aperture of the microscope filters the various transversal wave vectors that can be detected. If we suppose propagation in air between sample and the objective and if the angular aperture of the objective is introduced we have the relation: $k_x \leq \frac{2\pi}{\lambda}\sin(\theta_A)$. Following Heisenberg, we choose for the width of the transversal component of the $\overrightarrow{k}$ vector its maximum value: $\delta k_x = \frac{2\pi}{\lambda}\sin(\theta_A)$. The inequality (13) immediately implies the Abbe-Rayleigh relation:

$$\delta x \geq \frac{\lambda}{\sin(\theta_A)} \tag{14}$$

The discrepancy between equations (1) and (14) equations are not important. They are caused by different definitions of width and resolution. Moreover, equation (1) corresponds to a circular geometry and incoherent illumination which is not the case of equation (14) where coherent illimination by a plane wave is used.

To enhance the resolution, to decrease δx, it is necessary to increase δk_x. For a conventional microscope that uses homogeneous waves, δk_x is limited by $\frac{2\pi}{\lambda}$ and the resolution of a conventional far-field microscope is larger than λ.

This limit can be bypassed by using evanescent waves. The transversal component of an evanescent wave is larger than $\frac{2\pi}{\lambda}$, so:

$$k_x \geq \frac{2\pi}{\lambda} \Longrightarrow \delta k_x \geq \frac{2\pi}{\lambda} \Longrightarrow \delta x \leq \lambda$$

The previous demonstration was firstly given by J.M. Vigoureux [102]. It clearly establishes that, by using evanescent waves, the Abbe-Rayleigh limit can be bypassed, but the Heisenberg relation (13) remains verified. However,

there is a price to obtain an enhancement of the resolution: we have to use evanescent waves that must be detected in the near-field region.

6 Optical Tunneling

6.1 Fresnel's evanescent wave

Total reflection is the phenomenon that is generally associated with the creation of an evanescent wave. We consider a plane interface (z=0) between vacuum (z>0) and a dielectric homogeneous and isotropic medium (z<0) with an optical index $n = \sqrt{\epsilon} > 1$. The plane of incidence is the (x-z) plane. The angle of incidence is θ_i. The wave vector of the incident and of the transmitted waves are respectively $\overrightarrow{k_i}$ and $\overrightarrow{k_t}$:

$$\overrightarrow{k_i} = (u_i, 0, w_i) \text{ with } u_i = n\frac{\omega}{c}\sin(\theta_i) \quad (15)$$

$$\overrightarrow{k_t} = (u_t, 0, w_t) \text{ with } u_t = \frac{\omega}{c}\sin(\theta_t) \quad (16)$$

The transmission through the interface does not change the parallel component of the wave vector (Descartes-Snell's laws). The transmitted wave vector has the same x-component than the incident one:

$$\left(\overrightarrow{k_i}\right)_x = \left(\overrightarrow{k_t}\right)_x \Longrightarrow n\sin(\theta_i) = \sin(\theta_t) \quad (17)$$

For a small angle of incidence, $\sin(\theta_t) < 1$, the angle of transmission remains a real angle and there is a plane homogeneous transmitted wave. But when the angle of incidence becomes larger than the critical one, the angle of transmission becomes complex:

$$\sin(\theta_i) > \sin(\theta_l) = \frac{1}{n} \Longrightarrow \sin(\theta_t) > 1 \quad (18)$$

This phenomenon is better described in terms of wave vectors. The z component of the wave transmitted wave vector is given by the dispersion equation:

$$\left(\overrightarrow{k_t}\right)_z = \sqrt{\frac{\omega^2}{c^2} - \left(\overrightarrow{k_t}\right)_x^2} = \frac{2\pi}{\lambda}\sqrt{1 - [n\sin(\theta_i)]^2} \quad (19)$$

When the angle of incidence is under the critical one, $\left(\overrightarrow{k_t}\right)_z$ is real and the transmitted plane wave is homogeneous. But above the critical angle,

$\left(\overrightarrow{k_t}\right)_z$ becomes pure imaginary and the transmitted wave is an evanescent wave. The decay length L_0 of this evanescent wave is:

$$L_0 = \frac{\lambda}{2\pi\sqrt{[n\sin(\theta_i)]^2 - 1}} \qquad (\theta_i > \theta_l) \quad (20)$$

This decay length, depends on the index and on the angle of incidence. L_0 is always smaller than λ but remains larger than $\lambda/10$.

Above the critical angle, $\left(\overrightarrow{k_t}\right)_x \geq \frac{2\pi}{\lambda}$. This property was effectively used in microscopy to obtain images with a resolution better than the Abbe-Rayleigh criterion. The Optical Tunneling Microscope of Guerra [51, 50] is a conventional far-field microscope, with an objective lens, but where the sample is illuminated by an evanescent wave. It leads to beautiful images, but the gain in resolution is always small, because $n\sin(\theta_i) < 2$. Let us notice than such a microscope works in air, without an immersion liquid, but the use of an evanescent wave seems to be equivalent to an immersion in an effective index $n\sin(\theta_i)$.

6.2 Optical Tunneling

For $\theta_i > \theta_t$, the z component of the wave vector of the transmitted wave is pure imaginary and, as describe above, the evanescent wave does not lead to an energy flow in the direction perpendicular to the interface. The incident energy is totally reflected, the relection coefficient is equal to one and no energy is transmitted. But the evanescent wave exits, its amplitude does not vanish and it can excite fluorescent molecules, it can be captured by another glass interface or a tip.

In the presence of a second interface, of a molecule or of a tip, a part of the incident energy is transmitted or diffracted. Consequently, the reflection coefficient is no longer equal to one, it corresponds to Attenuated Total Reflection (ATR) or Frustated Total Internal Reflection (FTIR) [105].

For two similar interfaces with the same index of refraction separated by an air gap of thickness e,the calculation of the transmission coefficient is a classical calculation of optical studies [105]:

$$T = \frac{1}{1 + \alpha\left[\sinh\left(e/L_0\right)\right]^2} \quad (21)$$

L_0 is the decay length of the evanescent wave (Equ. 20). The coefficient

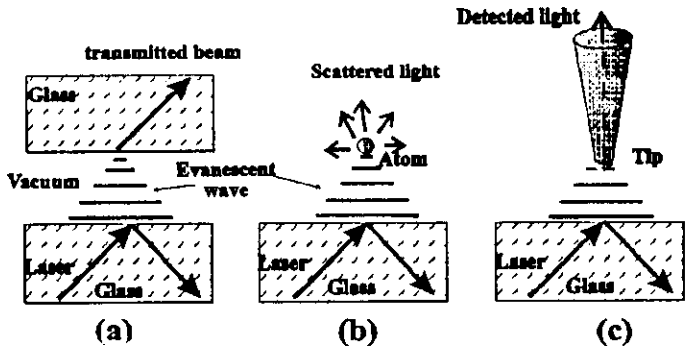

Figure 4: Optical tunneling: it is the transformation of an evanescent wave into propagating ones by another interface, by diffraction on an atom or a tip.

α depends on the polarization.

$$\alpha_{TE} = \left(\frac{n^2-1}{2n}\right)^2 \frac{1}{\cos^2(\theta_i)\left[n^2\sin^2(\theta_i)-1\right]} \quad \text{for TE or s polarization} \quad (22)$$

$$\alpha_{TM} = \alpha_{TE}\left[\left(n^2+1\right)\sin^2(\theta_i)-1\right]^2 \quad \text{for TM or p polarization}$$

7 Near-Field and Far-field: two examples

7.1 Radiating dipole

Let us consider a radiating dipole $\overrightarrow{d} = \overrightarrow{d_0}e^{-i\omega t}$ located at the coordinates origin. Such a dipole can be induced on a small polarizable system (atom, molecule, small sphere, tip apex) under the influence of an incident field $\overrightarrow{E_i}$: $\overrightarrow{d} = \overleftrightarrow{\alpha}.\overrightarrow{E_i}$.

By using Maxwell equations the radiated field can be easily calculated at any distance [20, 57]. If the dipole is suppose to be parallel to the z axis we obtain in spherical coordinates (r, θ, ϕ) and in MKSA units:

$$E_r(r,\theta,\phi) = \frac{2\cos(\theta)d_0}{4\pi\epsilon_0}\left(\frac{1}{r^3}-\frac{i\omega}{cr^2}\right)\exp\left[-i\omega(t-r/c)\right] \quad (23)$$

$$E_\theta(r,\theta,\phi) = \frac{2\sin(\theta)d_0}{4\pi\epsilon_0}\left(\frac{1}{r^3}-\frac{i\omega}{cr^2}-\frac{\omega^2}{rc^2}\right)\exp\left[-i\omega(t-r/c)\right]$$

$$B_\phi(r,\theta,\phi) = \frac{\mu_0\sin(\theta)d_0}{4\pi}\left(-\frac{i\omega}{r^2}-\frac{\omega^2}{rc}\right)\exp\left[-i\omega(t-r/c)\right]$$

$$B_r = B_\theta = E_\phi = 0$$

The electric field is always in the meridian plane (plane $\overrightarrow{r}-\overrightarrow{d}$). It has a has a longitudinal component (parallel to $\overrightarrow{r}$). It contains a far-field term (1/r), a near-field term ($1/r^3$) and an intermediate term ($1/r^2$). The magnetic field is always transverse (perpendicular to $\overrightarrow{r}$) and contains a far-field term in 1/r and a term in$1/r^2$.

The near-field terms, in the region $\frac{\omega r}{c} << 1$, the electric field, apart from its oscillation in time, is just the static electric dipole field. The magnetic field is a factor $\frac{\omega r}{c^2}$ smaller than the electric field:

$$\overrightarrow{E} = \frac{\left[3\overrightarrow{n}\left(\overrightarrow{n}.\overrightarrow{d}\right)-\overrightarrow{d}\right]}{4\pi\epsilon_0 r^3}\exp\left[-i\omega(t-r/c)\right] \qquad \left(\overrightarrow{n}=\frac{\overrightarrow{r}}{r}\right) \quad (24)$$

$$c\overrightarrow{B} = i\frac{\omega}{c}\left(\overrightarrow{n}\wedge\overrightarrow{d}\right)\frac{\mu_0}{4\pi r^2}\exp\left[-i\omega(t-r/c)\right]$$

In the far-field region, $\frac{\omega r}{c} << 1$, only the 1/r terms have to be kept and the fields take on the limiting forms,

$$c\overrightarrow{B} = \left(\frac{\omega}{c}\right)^2\left(\overrightarrow{n}\wedge\overrightarrow{d}\right)\frac{1}{4\pi\epsilon_0 r}\exp\left[-i\omega(t-r/c)\right] \quad (25)$$

$$\overrightarrow{E} = c\overrightarrow{B}\wedge\overrightarrow{n}$$

showing the typical structure of radiation field: $\overrightarrow{E}$ and $\overrightarrow{B}$ are transverse, perpendicular and with $E = cB$.

Moreover, using the fields expressions (23), it can be easily shown that only the far-field (1/r terms) contributes to the time averaged Poynting vector:

$$\left\langle\overrightarrow{P}\right\rangle = \frac{\overrightarrow{n}}{32\pi\epsilon_0 c^3}\left[\frac{\omega^2 d_0\sin(\theta)}{r}\right]^2 \quad (26)$$

Which leads to a radial flux of energy. The $1/r^2$ variations of the Poynting vector correspond to energy conservation: the total power radiated by the dipole is independent of r:

$$I = \frac{\omega^4 d_0^2}{12\pi\epsilon_0 c^3} \tag{27}$$

The near-field terms and the intermediate ones do not contribute to the time averaged Poynting vector.

7.2 Diffraction theory

Diffraction theory gives us another approach to near-field and Far-field notions. Let us consider, for example, a monochromatic wave E_i incident on a aperture on a thin opaque screen $\sum$.

In a scalar approximation, the diffracted field at point M can be calculated with the Huyghens-Fresnel principle [20, 57]:

$$E(M) = F \iint_{\Sigma} t(P) E_i(P) \frac{\exp[i\omega PM/c]}{PM} d\vec{P} \tag{28}$$

Each point P of the aperture, $\vec{OP} = (x, y, 0) = \vec{r}$, is source of a spherical wave. The total field at a point M, arises from the superposition of all these wavelets. The complex amplitude of each spherical wavelet is proportional to the incident amplitude at P, to the transmission coefficient of the aperture t(P). F is an universal constant that was determined by Fresnel: $F = \frac{-2i\pi}{\lambda}$.

With equation (28) and within the scalar approximation, the diffracted field can be evaluated at any distance from the diffracting plane $\sum$.

Until recent years, at optical frequencies, the measurement were impossible in the near-field region ($\omega PM/c << 1$) but only in the far-field region. So, by introducing the expansion:

$$PM = R + \frac{r^2}{2R} - \frac{\vec{r}.\vec{R}}{R} + ... \tag{29}$$

With $R = OM$. Equation (28) can be transformed to a simpler equation given by Fresnel, which expresses the diffracted field far from the screen $\sum$:

$$E(M) \simeq \frac{Fe^{i\omega R/c}}{R} \iint_{\Sigma} t(P) E_i(P) \exp\left[\frac{i\omega}{c}\left(\frac{r^2}{2R} - \frac{\vec{r}.\vec{R}}{R}\right)\right] d\vec{P} \tag{30}$$

Moreover, if the point M is going to infinity, Fraunhofer diffraction is obtained asymptotically from Fresnel's equation (30). The diffracted amplitude,

in the direction $\vec{R}$, is proportional to the Fourier transform of the field amplitude in the aperture. By introducing the spacial frequency $\frac{\omega}{c}\frac{\vec{R}}{R} = (u, v)$, we have:

$$E(M) = E(u, v) \simeq \frac{Fe^{i\omega R/c}}{R} \iint_{\Sigma} t(P) E_i(P) \exp\left[-\frac{i\omega}{c}\frac{\vec{r}.\vec{R}}{R}\right] d\vec{r} \tag{31}$$

In the Fraunhofer region, at an infinite distance from the diffracting screen, the diffracted amplitude is proportional to the Fourier Transform of the field amplitude in the z=0 plane.

8 Diffraction and evanescent waves. Plane Wave Expansion

The concepts of near-field and far-field were introduced long ago, in the context of radiation theory and diffraction theory and they are found on a decomposition into spherical waves. No evanescent waves appear in those descriptions. Those formalisms are not well adapted to theoretical discussion about near-field optics, and resolution limit. The formalism of the "plane wave spectrum" is much more interesting as it introduces Fourier transforms at any distance and not only in the Fraunhofer region. It is well adapted to resolution problems as it uses the spatial spectrum of the sample.

In this chapter, to simplify the discussion, we only consider a scalar theory, without any polarization. The field is one of the component of $\vec{E}$ or $\vec{B}$.

8.1 Plane Wave Expansion[98, 83]

We suppose that the field amplitude is known in the plane z=0: $E_0(x, y)$. The problem is to calculate the field amplitude, $E(x, y, z)$ in the half space z>0.

If we consider a radiation problem, $E_0(x, y)$ is created by sources that are located in the other half space z<0. For a diffraction problem, $E_0(x, y)$ is the field in the diffraction plane $\sum$. It is related to the incident field by a transmission coefficient:

$$E_0(x, y) = t(x, y) E_i(x, y, z = 0) \tag{32}$$

The field in the z=0 plane is a function of two variables and can be expressed as a 2D Fourier transform:

$$E_0(x,y) = \frac{1}{4\pi^2}\iint_{-\infty}^{+\infty} F(u,v)\exp\left[i\left(ux+vy\right)\right]dudv \tag{33}$$

$$F(u,v) = \iint_{-\infty}^{+\infty} E_0(x,y)\exp\left[-i\left(ux+vy\right)\right]dudv \tag{34}$$

For the Fourier Transforms, we use the notations of Champeney [23]. $F(u,v)$ is the spatial spectrum of the field in the plane $\sum$. In the general case, the integrations in (33) are without restrictions and runs from -∞ to +∞ over all the range of the spatial frequencies $u$and v. Properties of Fourier transforms are well known. The large structures of the field are associated to low spatial frequencies and the small details to high frequencies. The extension of the field $E_0(x,y)$ in space can be defined by two widths δx and δy, consequently the widths of F(u,v) in Fourier space are δk_x and δk_y. The widths are related by the relations:

$$\delta x\delta k_x \geq 2\pi \qquad \delta y\delta k_y \geq 2\pi \tag{35}$$

It can be demonstrated that the field for z>0 can also be expressed as a 2D Fourier spectrum

$$E(x,y,z) = \frac{1}{4\pi^2}\iint_{-\infty}^{+\infty} F(u,v)\exp\left(+iz\sqrt{\frac{\omega^2}{c^2}-u^2-v^2}\right)\exp\left[i\left(ux+vy\right)\right]dudv \tag{36}$$

It can be easily verified that the previous equation verifies the Helmoltz equation (4) and the boundary condition:

$$E(x,y,z=0) = E_0(x,y) \tag{37}$$

Thus, if the field is known in the z=0 plane, equation (36) leads to a rigorous expression of the diffracted field every where in the half space z>0.

If we introduce the 3D vector $\overrightarrow{k} = (u,v,w)$ with $w = \sqrt{\frac{\omega^2}{c^2}-u^2-v^2}$, equation (36) can be written:

$$E(x,y,z) = \frac{1}{4\pi^2}\iint_{-\infty}^{+\infty} F(u,v)\exp\left[i\,\overrightarrow{k}.\overrightarrow{r}\right]dudv \tag{38}$$

The vector $\overrightarrow{k}$ verifies the dispersion equation in vacuum. The diffracted field is thus rigorously expressed as a sum of plane waves, each wave is characterized by its amplitude $F(u,v)$ and its wave vector , $\overrightarrow{k} = (u,v,w)$. The summation is a 2D integration over spatial frequencies u and v that can be associated and the integrals (36,38) are called **Plane Wave Expansion** or **Angular Spectrum** representation.

The integrals contains both homogeneous and evanescent waves. For the low spatial frequencies ($u^2+v^2 \leq \frac{\omega^2}{c^2}$), w and the wave vector $\overrightarrow{k}$ are real. The corresponding plane waves are homogeneous and are propagating along $\overrightarrow{k}$. But, for high spatial frequencies ($u^2+v^2 \geq \frac{\omega^2}{c^2}$) w becomes pure imaginary and the plane waves are evanescent and they exponentially decaying along the z axis.

$$\boxed{u^2+v^2 \leq \frac{\omega^2}{c^2} \Longrightarrow w=\sqrt{\frac{\omega^2}{c^2}-u^2-v^2}\text{ real: }\textbf{homogeneous plane wave}}$$
$$\boxed{u^2+v^2 \geq \frac{\omega^2}{c^2} \Longrightarrow w=i\sqrt{+u^2+v^2-\frac{\omega^2}{c^2}}\text{ pure imaginary: }\textbf{evanescent plane wave}} \tag{39}$$

Integrations in (Equs. 36,38) are only restricted by the shape of the spectrum F(u,v) and not by the Snell-Descartes's laws. So, **contrarily to internal total reflection, diffraction can produce evanescent waves with very large values of the transversal wave vector (u,v).**

8.2 Influence of propagation on the Plane Wave Expansion of the field

The integral (36) is a 2D Fourier transform, the spatial spectrum of the field for z>0 is:

$$F(u,v,z) = F(u,v)\exp(+izw) = F(u,v)\exp\left(+iz\sqrt{\frac{\omega^2}{c^2}-u^2-v^2}\right) \tag{40}$$

It is proportional to the Fourier spectrum of the field for z=0 multiplied by the filtering function $\exp(+izw)$. For low spatial frequency, w is real, the exponential has 1 for modulus. In this case the filtering function is a simple phase shift and no information is lost by propagation. But as the phase shift depends on the spatial frequency, the field for z>0 can be strongly different from $E_0(x,y)$: that leads to Fresnel or Fraunhofer diffraction.

For high spatial frequencies, w is pure imaginary, the exponential becomes a decaying function of z. High spatial frequency can be strongly attenuated and in a real experiment can become smaller than the noise and can be non detected.

Propagation along the z axis attenuates the high spatial frequencies. It acts as a low pass filtering.

This last property is very important for understanding the influence of tip-sample distance on the resolution of SNOM and STOM.

8.3 Far-field and near-field microscopy

For a large object, δx and $\delta y >> \lambda$, thus δk_x and $\delta k_y << \frac{2\pi}{\lambda}$ and in the plane wave expansion of the diffracted field the amplitudes of the evanescent waves vanish or are negligible. For such a sample the far-field contains all the significant spatial frequencies and a far-field microscope can reproduce the object without any deformation. When the sample widths decrease the evanescent part of the sample spectrum becomes significant but they cannot be far-field detected and the image obtained by far-field microscope are strongly deformed (low pass filtering). When δx and $\delta y < \lambda$ we have δk_x and $\delta k_y > \frac{2\pi}{\lambda}$ and consequently most of the spatial spectrum of the sample is evanescent and we cannot obtain an image with a far-field microscope.

For a sub-lamda sample a near-field microscope must be used. But by immersing a probe in the near-field above the sample we can pick up and collect the information on small details that it transports.

In this king of near-field microscope (STOM) the probe is used to convert by diffraction the evanescent waves into homogeneous ones that are thus guided to the detector.

To understand the principle of a SNOM where the tip is used in the emission mode, we have only to apply the reciprocity principle to the previous argument. The incident light is guided from the source to the tip. The tip is a very small object that diffracts the incident light into a field that contains many evanescent waves with high spatial frequencies. By illuminating the sample by such a light, the evanescent waves are diffracted and transformed into propagating homogeneous waves that can be far-field detected.

The near-field microscopes in the emission mode or in the detection mode works with the same principle: transformation of evanescent waves into propagating ones.

8.4 Tip-sample distance and resolution

In conventional microscopy, the resolution depends on the numerical aperture of the objective and on the wavelength. In near-field microscopy the tip-sample distance is a fundamental parameter that has a major influence on the transversal resolution.

For near-field microscopes where the tip is used in the detection mode, the near-field above the sample can be expressed as an plane wave expansion (36). To resolve a detail of width δ, the plane waves with transversal wave vector $k_t = \sqrt{u^2 + v^2} \approx \frac{2\pi}{\delta}$ have to be detected. If δ is smaller than λ, those spatial frequencies correspond to evanescent waves. The damping length is given by the modulus of k_z:

$$L_\delta = \frac{1}{|k_z|} = \frac{1}{\sqrt{u^2 + v^2 - \left(\frac{2\pi}{\lambda}\right)^2}} \approx \frac{1}{\sqrt{\left(\frac{2\pi}{\delta}\right)^2 - \left(\frac{2\pi}{\lambda}\right)^2}} \approx \frac{\delta}{2\pi} \qquad (41)$$

Moreover, when $\delta << \lambda$ (practically $\delta < \lambda/3$), the decay length becomes independent of the wavelength and only depends on the detail width.

To resolve an object smaller than the wavelength and width δ, the amplitude of the evanescent wave must not be to small and the tip have to be at a distance that can be estimated by L_δ.

So, for a near-field microscope the resolution depends on tip-sample distance. Smaller is the object to be resolved, smaller must be the tip-sample distance. For an object of 100 nm, the tip distance must be around 20 nm. To obtain a good images of the object higher harmonics must be detected and tip sample distance as to be smaller than L_δ.

A similar discussion can be performed for the other kinds of near-field microscopes (SNOM in the emission mode, Reflection-SNOM, Perturbation-SNOM) and the conclusions are the same: the resolution strongly depends on tip-sample distance. The distance must be very small, a few nanometers are necessary to obtain images of $\lambda/10$ details.

This point has important technological consequences. The sample must be flat, the tip sample distance must be adjusted, controlled and stabilized with high precision (piezoelectric actuators are necessary).

Other parameters have an influence on the resolution. The other important one is the tip diameter. But a theoretical discussion of this point needs very complicated calculations and is already under study.

8.5 Relation between Plane Wave Expansion and usual diffraction theories

Diffraction theories generally use spherical wave expansion of the fields and evanescent waves do not appear in those formalisms. But a theorem given by Weyl in 1919 [98, 83] expands a spherical wave into plane waves:

$$\frac{\exp[ikr]}{r} = \frac{i}{2\pi}\iint_{-\infty}^{+\infty} \frac{\exp[i(ux+vy+i|w|z)]}{w} du dv \qquad (42)$$

with $r = \sqrt{x^2+y^2+z^2}$ and $k = \frac{\omega}{c}$.

The previous equation is a true plane wave spectrum of a spherical wave into plane waves and contains both homogeneous and evanescent plane waves and it can be said that evanescent waves are virtually contained into spherical ones.

With this theorem it is easy to obtain a demonstration of the Huyghens-Fresnel principle. By introducing the definition (34) of $F(u,v)$ into (3) and by derivation of equation (42) versus z we can express the field for z>0 versus the field in plane $\sum$:

$$E(x,y,z) = -\frac{1}{2\pi}\iint_{\Sigma} E_0(x,y)\frac{\partial}{\partial z}\left[\frac{\exp[ikr]}{r}\right] dxdy \qquad (43)$$

$$E(x,y,z) = -\frac{ik}{2\pi}\iint_{\Sigma} E_0(x,y)\frac{\exp[ikr]}{r}\left[\frac{z}{r}\left(1+\frac{i}{kr}\right)\right] dxdy$$

This expression was given by Rayleigh in 1897, it is called the first Rayleigh-Sommerfeld diffraction equation ([98] and [83] page 192) and it corresponds to a Dirichlet condition for diffraction problems. It is a rigorous expression of the diffracted field versus the field in the z=0 plane.

It contains the Fresnel factor, $-\frac{ik}{2\pi}$, and for large distance ($kr >> 1$) and observation close to the z axis ($z/r \simeq 1$) it leads to the Huyghens-Fresnel expression (28).

Let us notice that there is a complete equivalence of the near-field concept and evanescent waves. A spherical wave contains both evanescent and homogeneous waves. So, the far-field of an oscillating dipole contains evanescent waves and the near-field contains homogeneous ones.

8.6 Asymptotic limit of a Plane Wave Expansion

The plane wave expansion (36) is a rigorous expression of the diffracted field that is valid at any point in the half space z>0. The calculations are simpler than in usual diffraction theory which uses a spherical wave expansion. Numerical algorithmes can be very efficient as Fast Fourier Transform can be used.

When a far-field value of the field is needed, an asymptotic approximation is necessary.

If we consider a plane wave expansion (36), the asymptotic limit when $r \to \infty$ in a fixed direction $\vec{n} = \frac{\vec{r}}{r}$ can be obtained by using the method of the stationary phase:

$$E(x,y,z) \underset{r\to\infty}{\approx} \frac{-ikn_z}{2\pi} F(kn_x, kn_y)\frac{\exp(ikr)}{r} \qquad (44)$$

The far-field limit is a spherical wave, the amplitude of which is proportional to the Fourier spectrum of the field in the z=0 plane calculated for the spatial frequency kn_x, kn_y. This point is another demonstration of the Fraunhofer expression of the diffracted field at very a large distance from the z=0 plane.

9 Simple models of Scanning Near-Field Microscopes

With the formalism described in the previous chapter we are now able to propose simple, pedagogical, models for near-field microscopes. A STOM working in the detection mode and a SNOM working in the emission mode.

9.1 A simple model of STOM

9.1.1 The model

The model is presented in (Fig.5). The sample is on the flat interface (z=0) of an hemispherical glass lens of index n. The sample is illuminated by a plane wave, propagating in glass, the angle of incidence is θ_i. The incident field can be written:

$$E_{inc}(x,y,z=0) = E_0 \exp\left[i\vec{k}_{inc}.\vec{r}\right] \qquad (45)$$

With $\vec{k}_{inc} = (u_{inc}, v_{inc}, w_{inc})$ and $\sqrt{(u_{inc})^2+(v_{inc})^2} = n\frac{\omega}{c}\sin(\theta_i)$.

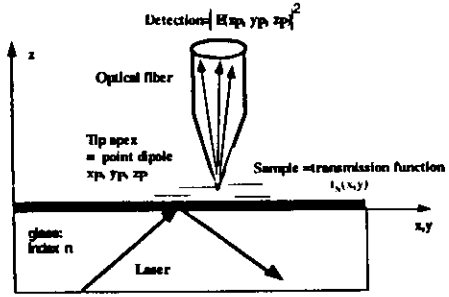

Figure 5: A simple model of STOM

The sample is characterized by its transmission function t(x,y). After the sample, the transmitted field in the z=0 plane is thus simply the product of the incident field by the transmission function:

$$E_0(x,y) = t(x,y)E_{inc}(x,y,z=0) = t(x,y)E_0 \exp[i\left((u_{inc}x + v_{inc}y\right) \quad (46)$$

The transmission function can be expressed as a 2D Fourier transform:

$$t_S(x,y) = E_0(x,y) = \frac{1}{4\pi^2}\iint_{-\infty}^{+\infty} T(u,v)\exp\left[i\left(ux+vy\right)\right]dudv$$

The probe is supposed to be a very thin tapered tip with a very small apex. The apex will be located at point $P = (x_P, y_P, z_P)$. It is supposed very small to be considered as a small dipolar sphere. Within this model, the detected intensity is simply proportional to the square modulus of the field at the apex position.

9.1.2 Calculation of the detected intensity

By using the result of previous chapter, the calculation of the field at the tip apex is very easy. We need the Fourier transform of $E_0(x,y)$:

$$F(u,v,z=0) = E_0 T(u-u_{inc}, v-v_{inc}) \quad (47)$$

Then the field for z>0 is a plane wave expansion:

$$E(x,y,z) = \frac{E_0}{4\pi^2}\iint_{-\infty}^{+\infty} T(u-u_{inc}, v-v_{inc})\exp\left[i\left(ux+vy+iwz\right)\right]dudv \quad (48)$$

and the detected intensity is simply:

$$I_D(x_P,y_P,z_P) = K\left|E(x_P,y_P,z_P)\right|^2 \approx \left|\iint_{-\infty}^{+\infty} T(u-u_{inc}, v-v_{inc})e^{\left[i\left(ux_P+vy_P+iwz_P\right)\right]}dudv\right| \quad (49)$$

In this model, the object is the transmission function $t_S(x,y)$ and a good microscope must lead to images that looks like the object.

For normal incidence ($u_{inc} = 0 = v_{inc}$) and for z=0 the field (48) is proportional to the transmission function and the image looks like the object. But this result is only a direct result of equation (47) and a consequence of the use of a crude model to describe the sample by a transmission coefficient.

For normal incidence and $z \neq 0$, the spatial spectrum of the field is filtered by the exponential factor $\exp[iwz]$ described above. It leads to a low pass filtering and it implies a very small tip-sample distance to detect significant spatial frequencies of the sample.

In (Fig.6) we have plotted STOM intensity maps I(x,z) calculated with previous equations. The sample is a 1D rectangular grating of period a and width b=a/2. The x axis is perpendicular to the grooves. The incident wavelength is $\lambda = 0.67\mu m$, the angle of incidence is above the critical one (n=1.5, $\theta_i = 45°$). For a period smaller than the wavelength (Fig. 6a) only evanescent waves are diffracted. The mean detected intensity is slowly decaying with a decay length given by L_0, the decay length of the Fresnel evanescent wave. The details have shorter decay lengths: for z=0, the sample profile is well reproduced. But soon (30 nm) higher harmonics are attenuated and only the fundamental exists. For z>50 nm the sample profile is a sin function.

For comparison, we have also plotted in (Fig. 6b) the same calculations for a grating period larger than the wave length. The same evolution is observed, very close to the sample high spatial frequencies are present, but when z is increased only low spatial frequencies are not attenuated. For $a=2\mu m$, few propagating plane waves are diffracted, their interferences can be seen in the plot.

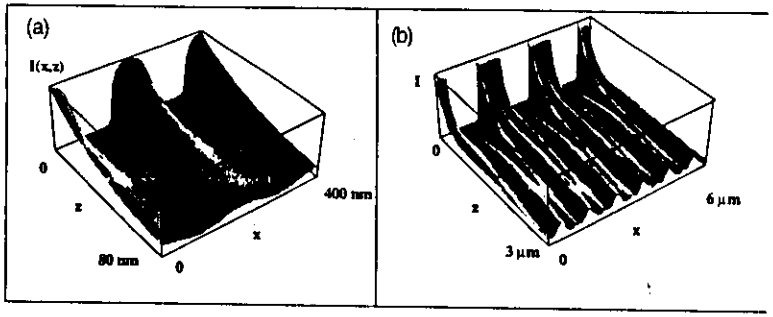

Figure 6: STOM intensity maps I(x,z) for a periodic grating. The wave length is $\lambda = 0.67\mu m$, the angle of incidence is 45°. a) grating period a=200 nm b) a=2μm

9.2 A simple model of SNOM

9.2.1 The model

The principle of the SNOM is presented in (Fig5). The sample is in the plane z=0 and it is also described by a transmission function t(x,y). But the sample is now illuminated by a nano-source that is located at point $P = (x_P, y_P, z_P)$ with $z_p < 0$. The diffracted field is far-field detected and we suppose that we use a detector that only detects the field into a small solid angle $\delta\Omega$ around one direction defined by the unitary vector $\overrightarrow{n_D}$.

9.2.2 The nano-source field

This source will be defined by its emitted field in a reference plane. If the apex of the probe is located at the origin of the coordinates, the emitted field by the probe in the plane z=0 is:

$$E_P(x, y, z = 0; x_P = 0, y_P = 0, z_P = 0) = \frac{1}{4\pi^2} \iint_{\Sigma} F_P(u, v) \exp\left[i\left(ux + vy\right)\right] dudv \tag{50}$$

The quality of the probe depends on the spatial spectrum $F_P(u, v)$. When the probe is located at point $P = (x_P, y_P, z_P)$, by using the theory of the plane wave spectrum explained above, it is easy to express the emitted field in the z=0 plane:

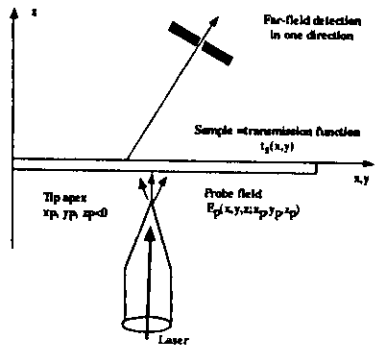

Figure 7: A simple model of SNOM

$$E_P(x, y, z = 0; x_P, y_P, z_P) = \frac{1}{4\pi^2} \iint_{\Sigma} F_P(u, v) \exp\left[i\left(u(x - x_p) + v(y - y_P) + w\left|z_P\right|\right)\right] dudv \tag{51a}$$

For the SNOM this field is the incident field on the sample and its Fourier transform is thus:

$$F_i(u, v) = F_P(u, v) \exp\left[-i\left(ux_p + vy_P\right) + iw\left|z_P\right|\right] \tag{52}$$

9.2.3 Calculation of the detected intensity

The field after the sample but in the z=0 plane is the product of the incident field by the transmission function (32). Thus the 2D Fourier transform of this field is a convolution product:

$$F(u, v; z = 0) = \frac{1}{4\pi^2} \iint_{\Sigma} T(u - u', v - v') F_i(u', v') du'dv' \tag{53}$$

By using once more the plane wave spectrum theory, the diffracted field above the sample can be written:

$$E(x, y, z > 0) = \frac{1}{4\pi^2} \iint_{-\infty}^{+\infty} F(u, v; z = 0) \exp\left[i\left(ux + vy + iwz\right)\right] dudv$$

The detector is located far from the sample and we must use the asymptotic expansion (44) to express the diffracted far-field in the direction of the detector. The far-field detected intensity can be written:

$$\frac{dI_D}{d\Omega} \approx (kn_z)^2 \left|F(kn_x, kn_y; z=0\right|^2 \tag{54}$$

The final expression is obtained by introducing the expression of the spatial spectrum (53)

$$\frac{dI_D}{d\Omega}(\overrightarrow{n}) \approx \left(\frac{kn_z}{4\pi^2}\right)^2 \left| \iint_\Sigma T(kn_x - u, kn_y - v) F_P(u,v) e^{[-i(ux_p+vy_P)+iw|z_P|}\, du dv \right|^2 \tag{55}$$

9.2.4 Discussion

The convolution product that appears in equation (55) theoretically explains the principle of SNOM. The sample details smaller than λ are associated with high spatial frequencies. If a propagating plane wave is used for illumination, they lead to evanescent waves that cannot be far-field detected. The tip alone is very small and its emission field is composed of non-radiative evanescent waves. But if the tip is used to illuminate the sample, the diffraction process implies a convolution product that combines high spatial frequencies of the sample and of the probe into low spatial frequencies that can be far-field detected.

Generally the detector is along the z axis and we have $n_x = n_y = 0$, in this case we obtain for the detected intensity:

$$\frac{dI_D}{d\Omega}(\overrightarrow{0}) \approx \left| \iint_\Sigma T(u,v) F_P(-u,-v) e^{[i(ux_p+vy_P)+iw|z_P|}\, du dv \right|^2 \tag{56}$$

The Fourier spectrum of the transmission coefficient is multiplied by 2 filtering coefficients. The exponential $\exp(+iw|z_P|)$ is caused by propagation and is a low pass filtering. The influence of tip quality is contained in its spatial spectrum, $F_P(-u,-v)$.

A efficient near-field tip must have an emitted field with many high spatial frequencies. The very thin tip does not have a filtering effect and its spatial spectrum could be supposed to be flat for any frequency: $F_P(u,v) = 1$.

The expression of the detected intensity obtained for the STOM where the tip is used in the detection mode and for the SNOM where the tip is used

in the emission mode are very similar and can be the same is a transmission function is associated to a real detection tip. This identity of results for the emission and detection modes can be demonstrated by using the reciprocity principle.

10 Technical problems and their solutions

The principle of local probe optical microscope is very simple but many technical problems have to be solved for carrying out experimental set-up. In this section we describe the most important points that are common to all the various configurations.

10.1 Scanning

All the local probe microscopes use piezoelectric actuators to move the tip in the 3 directions of space. Tripod structures as well as tube scanners are used in near-field optical microscopes. A nanometric resolution in x and y is enough for most of the experiments. In the z direction, that corresponds to the tip approach a better resolution is necessary. Commercial nano-drive actuators can be found. The scanning quality depends on the quality of the materials: linearity and a small hysteresis are necessary. Moreover, the quality of the electronic is also important. It must have a very high signal to noise ratio in order to avoid tip position fluctuation and it must balance the non-linearity and the hysteresis defects. A compensation of thermal drift is also necessary.

The coarse-grained displacements for the tip approach are obtained by using an auxiliary micropositning stage. For this purpose mechanical system combined with piezo "pushers" with a large travel can be used.

10.2 Vibration isolation

Filtering of mechanical vibration is necessary to obtain high resolved images. But it is a difficult problem that is common to all the local probe microscopies. The desired resolution determines the length to which vibration damping must be achieved. A good rule of thumb is to require a stability of at least one order of magnitude better than the wanted resolution.

First the microscope must be shielded from the external vibrations. The mechanical vibrations can be filtered by a special stage. It is also important to isolate the microscope from air vibrations.

A very efficient damping is obtained for high frequencies but vibration isolation is less efficient for low frequencies (0.1-10Hz). So, the near-field microscope must be designed to have high resonance frequencies so that to prevent a resonance with an external low frequency. The microscope must be compact, rigid and build with low-mass components.

10.3 Light sources

A large variety of light sources can be used in near-field optical microscopy: conventional sources, photodiode, laser-diode, laser. Most SNOM configurations utilizes CW lasers as light sources because a laser beam can easily and efficiently be coupled into an optical fiber. The output power is around a few mW. Higher power could be useful to obtain higher signal-to-noise ratios and should be necessary for spectroscopic applications. But for SNOM working in the emission mode, the input power is limited by thermal damages on the tip apex and on the sample.

For time delay measurement or time resolved spectroscopy pulsed laser can be used.

10.4 Detection

Detection is the transformation of collected light into an electric signal. Many near-field optical experiments have enough collected light and a simple photodiode can be used for detection. The signal-to-noise ratio can be strongly enhanced by utilizing a photomultiplier tube (PM). A PM is more sensitive at room temperature and when properly cooled it can be used for single photon detection. A cooled CCD detector is an appropriate choice for spectroscopic applications. A complete spectrum of low intensity can be acquired in a parallel fashion more rapidly than with a PM and without having to scan the grating.

Many experiments are performed with continuous light source. To improve the signal-to-noise ratio it can be useful to modulate the incident light and to utilize a lock-in amplifier.

10.5 Control of tip position

As explained in the theoretical chapters, the detected intensity depends strongly of tip position. The tip must be at a few nanometers from the sample and the resolution is rapidly degraded when the tip-sample separation is increased. Thus, it is necessary to stabilize and control the tip position along the z axis at a very high level of precision.

This problem is common to all the local probe microscopy but near-field optical microscopy has specific difficulties.

In STM, the tunneling current shows an exponential decay when tip separation is increased. It can be used as a as a feedback signal to control tip position. The optical equivalent of the STM is the STOM. In this configuration, the signal collected by the optical fiber is also an exponential decaying function and it can be used as a feedback signal.

In the other near-field optical microscopes (SNOM, R-SNOM, Perturbation SNOM) the optical signal is not a monotonous function of tip-sample separation and another signal must be used to control tip position.

For metallic (or metallized) tip and conducting samples it is possible to perform a STM and a SNOM experiments simultaneously. The electronic tunneling current is used as a feedback signal.

Another proposed solution to the tip control problem, is to couple a scanning force microscope and a near-field optical microscope [3, 82]. The same tip is used as a bifunctional probe, as a force and an optical sensor. This combined microscope is very interesting as it produces simultaneously an optical image and an AFM image, that could lead to fruitful comparisons between the optical signal and sample topography.

Many current near-field microscopes use "shear-force" signal to maintain a constant tip separation [13]. The fiber is dithered laterally at a resonant frequency. As the tip is brought in the vicinity of the sample (z<20 nm) the tip amplitude is damped by shear-forces between the tip and sample. The exact nature of the force is unknown but this phenomena gives a very simple and efficient feedback signal. By maintaining a constant dithering amplitude for tip oscillation a constant tip-sample separation is supposed to be maintained. Generally the oscillation are optically measured by using an transversal light beam.

10.6 Probe fabrication

10.6.1 Tapered optical fiber

Today most of the near-field optical microscopes use a tapered optical fiber: the apex of the tip is the optical probe and the optical fiber is employed to guide the light of the source in the emission mode or to guide the detected light in the collection mode. The taper can be obtained from a monomode optical fiber by two different processes.

The first method is a **chemical etching** of the fiber in a solution that contains ammonium fluoride buffered hydrofluoric acid. The etching of the cladding is faster than that of the core, so that the cladding is removed and

the core becomes conical. In [87] the description of this process is detailed and images of tips are presented. The composition and the concentration of the etching solution, the etching time and the doping concentration of the core of the fiber have an influence on the size and shape of the taper. Tapers with tip diameters around 20 nm and cone angles on the order of 25° can reproducibly be fabricated by this method.

The second method is a physical process. It involves a **heating and pulling** process and it was derived from microbiologists who, for many years, have pulled pipettes to quite small radii. It can also be considered as a modification of the method used for the fabrication of optical fibers except that it runs to breakup. The heating operation can be performed with a gas burner, or with an electric arc, or by irradiation with an infrared laser.

Commercial apparatus are available. The shape and size of the tip depends on the precise details of the heating, pulling and cooling times. A methodical description of this method in presented in [101].

The two methods obtain similar results: conical tapers with tip diameters around 20 nm can reproducibly be fabricated.

It is possible to use the tapers without any other treatment. Such **uncoated tips** are generally used in collection mode near-field microscopes and they have provided images with high lateral resolution.

But it is also possible to use metallized tip. The naked taper obtained by one of the methods described above is coated by aluminium in a vacuum chamber. The metallization is performed transversely on a spinning tilted tip in order to obtain a small circular uncoated aperture at the end part of the tip. The diameter of the aperture can be as small as 20 nm. This kind of tip is called a **small aperture tip** and it achieves the idea of Synge for the optical probe: a small aperture in a perfect metallic screen.

10.6.2 Other tips

Some scanning force (SFM) microscopes uses a dielectric tip as a force sensor. This tip, generally in Si_3N_4, are transparent and they can be used also as an optical probe. As mentioned Such kind of tips can be used to build combined SFM-STOM microscopes [3, 82].

Near-field optical microscopes working in the perturbation mode do not need a transparent tip because the tip is not used for propagating light. Consequently, STM metallic tips can be used. They are in tungsten and can be thinner than dielectric tappers. Fineness at the atomic scale is easily reached that explains the very high resolution obtained by this kind of microscope.

10.6.3 Alternative probes

In order to enhance the efficiency of light emission or light detection alternative probes have been proposed and tested.

A coaxial structure, with a metallic core is a waveguide without any cutoff and could have a high efficiency. Several groups have considered this configuration in near-field microscopy[35, 60]. The construction of such a structure, glass fiber with a silver core, is easy in far infrared and more difficult in the visible region.

U. Fischer proposed to use a tetrahedral tip [33]. It is made from a corner of ultramicrotome blade and a waveguide is made by evaporating metal on two adjacent faces. It seems that a nanometric resolution was reached with the tetrahedral tip.

Danzelbrink et al. [25] construct a tetrahedral tip made in cleaved monocrystal of AsGA. The use of a crystalline semiconductor is very interesting. First very sharp and well defined edges can be obtained. Secondly, the optoelectronic conversion can be obtained in the probe itself.

It is also possible to put fluorescent molecules at the apex of a tip. The molecules can amplify or guide the light. Moreover, photochemical reactions are sensible to the variations of Ph or RedOx potentials. Those photochemical nanoprobe could be very useful in biological applications [61].

11 Results and Applications

11.1 Resolution limits

Many groups have succeeded to build near-field microscopes working in the emission mode or the collection one that readily provide images with a lateral resolution around 50 nm. By using these configurations, the ultimate resolution seems close to 15-20 nm. In reference [17] are shown beautiful images obtained with a SNOM using a small aperture tip and a resolution of 15 nm is demonstrated. A similar resolution limit is obtained with a STOM configuration an a dielectric tip without coating [4].

The origin of this 15-20 nm resolution limit is not to be found in a theoretical reason but it has a technological nature. The optical fiber are made with an amorphous material and, today, it seems impossible with this material to fabricate a tip with a radius of curvature smaller than 15-20 nm.

As mentioned above a near-field microscope working in the perturbation mode reached in 1995 a lateral resolution of 1 nm [104]. This important result was obtained by using a STM tungsten tip that is sharp at the atomic scale.

The lateral resolutions of the various configurations of near-field microscopes are worse than the resolution of a conventional electronic microscope or of a STM or of a SFM. However, even with a restricted resolution around 20 nm, the future of optical near-field microscopy is fully open: it is currently possible to extend in the sub-micron domain all the many applications of conventional optics and microscopy, all the optical methods of analysis, measurements and fabrication. Consequently, within the past two years, many papers, that demonstrate real applications of near-field optics, have been published.

11.2 Spectroscopies

In conventional microscopy it is very difficult to change the wavelength. In the visible region many transparent materials with different indices can be used to build lenses and the aberrations can be corrected. It is not possible in the ultraviolet or in the infrared domains where only few transparent materials can be found.

This problem is less important in near-field microscopy that does not need a lens to obtain images. Optical fibers for the infrared and the ultraviolet regions are available and it is then easy to fabricate tapered tip for these wavelengths.

Near-field microscopes working in the perturbation mode do not need a transparent tip. With this kind of microscope it is easy to change the wavelength. C. Boccara [19] could observed 0.015 μm details on a gold film illuminated by Co_2 laser with λ =10 μm.

For simple imagery applications it could be useful to change the wavelength in order to enhance the contrast of some details of the sample. At a different wavelength a part of an object can have a different absorption or scattering cross section. For the same purpose it is also possible to use the specific fluorescence of some chromophore. In biology the fluorescent labelling methods can be extended without any difficulty in near-field microscopy [16, 12]. A simple filter is able to separate the various different biological part of a sample.

Moreover by adding a real spectroscope to a near-field microscope it is possible to extend in the nanometric domain all the possibilities of chemical analysis by optical spectroscopy. These applications are not possible by others local probe microscopies as the STM or the AFM.

But to obtain a spectrum at one point of an image or spectroscopic images of a sample it supposes that enough luminous energy can reach the detector. For spectroscopic applications, many parts of the near-field apparatus have to be optimized: efficiency of the fiber, efficiency of the collection optics,

coupling with the spectroscope, quantum yield of the detector...

These problems have been solved by some groups. For solid state spectroscopic studies Betzig et al. have designed a spectroscopic SNOM [49]. The sample is in a high-vacuum cryostat that can work from room temperature to liquid Helium temperature. They have studied quantum dots structures [48] and have observed single molecules [11]. The Another group have succeeded to image and to take a spectrum of two similar molecules located at two different sites [81]. By measuring the time decay of fluorescent light, experiments of time resolved spectroscopy have been obtained in near-field microscopy on ruby micro-crystallites [88] and on single molecules [31].

Piednoir et al; used a STOM to obtain the first infrared spectra [89]. They used a special fluoride optical fiber with a tip diameter of 1 μm. The characteristic doublet of a photoresin deposited on a Si substrate is clearly observed with a spectral resolution of 5 cm^{-1} and they compared the spectra of the same sample in far-field and in near-field.

The first Raman spectra have been obtained shown in 1997 at the international conference on near-field optics at Jerusalem and will be published soon.

11.3 Local studies of optical components

Many optical components and systems have lengths around the wavelength and a near-field microscope in the detection mode is a very suitable tool to measure in-situ and in real-time the structure of the fields and to verify the good running. Very often, these studies are impossible by far-field methods.

Optical waveguides have evanescent waves on their structures that can be collected by an optical probe and that are associated with the propagating modes inside. Direct observation of TM and TE modal field distribution, mode beating and observation of a Y-junction is presented in [54].

[100] used a SNOM to study rare earth doped optical fibers. These devices are utilized for light amplification and the local modifications in the density of Erbium atoms can significantly affect the performances. By a SNOM luminescence measurement, with a sub-micron resolution, spreading of the doping in the cladding can thus be demonstrated.

The optical probe can also be used to map the emitted field at the end part of a quantum well laser [22]. Recently O. Marti have proposed a very interesting study of a working laser diode. The optical probe is immersed in the emitted near-field. A spectroscope analyses the light and so the various modes can be spectrally separated. The near-field spectroscopy leads to map of the emitted field for each mode versus the diode current [53]

11.4 Magneto-optical materials and mass storage

Magneto-optical material are used to build mass storage systems. In existing systems, writing and reading of data are performed by using a small light spot. The maximum density of information is thus limited by diffraction. With a red light a bit has a width of 1 μm. In a few years, blue diodes will be used and the light spot will be twice smaller. Near-field techniques could be able to strongly enhance the density of integration.

With a STOM configuration, a group has succeeded to image domain structure and to observe nanometric details related to walls movements [95]. E. Betzig [18] uses a SNOM configuration to read patterns written by far-field method. But a tip used in the emission mode can also be used for writing. At the end part of a small aperture tip there is a high density of energy that is partly absorbed by the metal. When the laser power is above 5 mW the absorption is enough to heat the tip at $200°C$. The sample is at few nanometers from and the thermal flux from the tip to the sample could be enough to heat the sample above the Curie temperature. The magnetization of the heated region is lost , after cooling it can get a magnetization in the opposite direction. With such a method a grating of 20X20 dots was written and read. The density of integration was around 7 gigabits/cm^2.

Other experiments are under developpement, they use a reflection-SNOM configuration. An important progress in speed of reading is necessary; to day it is limited to 10 kHz.

11.5 Photolithography

Far-field photolithography is the method that is at the present time used for patterning the masks of integrated circuits. The key parameter is also the imaging resolution, it is presently in the sub-micron domain. Sharpening the features requires to use a smaller wavelength (from 0.5 to 0.35 or 0.2 μm) but this evolution is difficult and expensive.

The energy at the apex of a near-field tip is large enough to induce a permanent sensitization of a conventional photoresist. Near-field optical technique could provide a cheap and flexible method, with visible light, to enhance the resolution. The first attempt to write a pattern in a photoresist (PMMA) film with a near-field probe was in a paper by Ferrell et al. [32]. Various methods of writing was suggested: mechanical indentation, thermomechanical indentation. New results were obtained more recently that demonstrated the possibility of creating lines or stuctures with a lateral resolution better than $\lambda/5$ (100 nm) by using photolithograpy. In the two experiments the photoresist is illuminated by a nano-probe but the created structure is imaged by a scanning force microscope [62] or a shear-force technique [26]. In the last paper, by using PMMA-DR1 from IBM, it is proposed a writing method without a developping step: a real time image of the modified surface is recorded.

11.6 Biology

The conventional far-field transmission or scanning electronic microscope is the technique that is used to obtain images of biological samples with a sub-micron resolution. But it implies strong constraints: samples must be dried, metallized and observed in a vacuum chamber. The observed samples are thus far-from biological conditions and can be damaged by the electron beam. The new local probe microscopies lead to new tools for studying biological samples. STM needs a sample metallization, SFM is a powerful tool that is extensively used. Near-field optical microscopy applications to biology are still in development but it seems to be very well adapted to biological applications. The interaction with light and the optical probe is rather soft and a near-field optical microscope can work in air or in water that open the possibility of in situ or in vivo studies.

The first images were produced in1993 [10]: fluorescent images of a lamellipodium from a fixed mouse fibroblast cell. Then, Van Hulst [54] presented the first application to fluorescence in situ hybridisation of human methaphase chromosome, where the localized fluorescence allows to identify specific DNA sequences. Images of virus T4 and of of filament of salmonella were also published [87].

Biological studies at a molecular scale have been demonstrated. Xie et al. [29] obtained fluorescent images images of proteins and of intact photosynthetic cellular membranes [30]. In the last paper they also produced spectra and lifetime measurements.

SFM and near-field optical microscopy are complementary instruments. A combined SFM-SNOM or SFM-STOM seems to be the ideal tool for biological applications. The SFM gives the topographic information, the optical microscopy can give simultaneously, an image or a fluorescent image of the same point.

12 Theoretical methods

The theoretical models presented above (chapter ??) are rather simplified and must be considered as a first pedagogical approach to the theory of near-field optics. They contain the main theoretical tools and they are able

to describe the main features of the phenomena. However they cannot lead to a realistic calculation of near-field images. The formalism presented above is found upon two approximations: a scalar theory to describe the field and a transmission function to describe the sample.

It is not difficult to overcome the first approximation. It is easy to use a vectorial plane wave expansion to described the diffracted electromagnetic field and the polarization properties of the incident and diffracted fields can be taken into account

In (chapter ??) a transmission function is used to describe the sample. This model is currently used in conventional microscopy, it is a good approximation for large sample width, but it is no longer valid when the sample width decreases and it is completely false in the sub-wavelength domain. **The concept of a transmission function is not valid for near-field models**, more rigorous theoretical approaches must be used that verify Maxwell equations and boundary conditions.

12.1 Classifications of theoretical schemes

A comparison of theoreticals models of near-field microscope can be found in two review papers [67, 42].

Most of the methods suppose a monochromatic incident waves and does not study the transient phenomena. However few papers have used a finite-difference scheme in the time domain to solve Maxwell equations [58, 59]. Such a method is purely numerical, it needs a very powerful computer with large memory even to study a very simple system.

To classify calculations that consider a monochromatic incident wave and use monochromatic Maxwell equations, we propose two criteria: microscopic or macroscopic theory, global or non-global theory.

12.1.1 Microscopic or macroscopic theory

For microscopic theories the sample and the tip are supposed to be composed of a set of discrete points scattering centers. These centers can be atoms or molecules, but generally they are artificial small polarizable centers, described by their polarizability (dipolar, quadrupolar or multipolar). Within a microscopic approach, the electromagnetic field verifies Maxwell equations in vacuum and there is no boundary conditions. Sample and tip are optically described by the arrangement and the nature of the scattering centers.

On the contrary, for macroscopic theories the sample and the tip are considered as continuous media that are optically decribed by macroscopic

parameters. The most important parameter is the dielectric constant (dielectric tensor for anisotropic or magnetic samples), but we can also consider the non-linear parameters, the magneto-optical constants, electro-optical constants...These theories used macroscopic Maxwell equation and the boundary conditions between two media must be satisfied.

12.1.2 Global or non-global theory

In principle, in a near-field calculation tip and sample are to be considered as a single diffractive object. A global theory takes the sample-tip coupling into account and do not neglect, a priori, the multiple scattering between tip and sample: calculations are performed into one step.

Non-global calculations are simpler. The tip-sample coupling is neglected and calculations can be performed in two steps.

For a SNOM working in a detection mode, the first step is to calculate the diffracted field by the sample. Then a model of tip detection is used to obtain the calculated image. In this case the tip is suppose to be a passive probe that only "measures" the near-field above the sample without any modifications. For a SNOM working in the emission mode, in a first step the field emitted by the tip is calculated. Then this field is used as an incident field on the sample and diffraction by the sample is calculated. In this case it is supposed that the sample does not modify the tip emission.

12.2 Coupled dipoles and multipoles methods

The first inclusive model of SNOM, that took into account the electromagnetic tip-sample coupling, utilized an artificial microscopic method [63, 44]: the **coupled dipoles method**. Tip and sample are discretized and supposed to be composed of a discrete series of scattering centers, dipolar or multipolar ones.

The coupled dipole method was firstly applied to study far-field diffraction of light by non spherical dielectric grains [93]. Ch. Girard has successfully applied this method to SNOM models. [63, 44, 41, 39, 21, 40]. The method has been enhanced by taking into account multipolar polarizabilities and propagators [38].

12.3 The multiple multipole method (MMP)

The multiple multipole method (MMP) was at first developped for antenna calculations in the radio-waves domain. Like the coupled dipole method, it

supposes that the diffracted field is created by a discrete series of multipolar field.

This method looks like the coupled dipole method, But it is not a microscopic theory as the field verifies the boundary conditions on the interfaces. For this purpose a lest square minimization method is used to determine the number of multipoles and of multipolar amplitudes. The method has a better convergence than the classical, one center, multipolar expansion. It is well adapted to near-field calculations [84] as MMP method can well described diffracted field above localized geometries. But the discretization of the diffracting system, sample and tip remains artificial and it is impossible to physically understand the meaning of the various multipoles. Moreover this method needs large computation memory and time. It was used to study tip emission and light confinement by Novotny and Pohl [85, 86].

12.4 Volume integral method

The macroscopic volume integral method was known many years ago and was applied to many diffraction problems. It is found upon Green's function formalism and can be transformed into a Lypman-Schwinger equation. The first application to SNOM were published in 1993 [28, 90]. For numerical constraints, they were limited to 2D samples and tip. Reference [90] is a beautiful study of the near-field scattered by subsurface particle. In [28] a global model of SNOM is presented. The tip is a 90° prisme edge and the near-field structure between tip and sample is studied.

Then this method was mostly used by Girard, Dereux and Martin. They study the light confinement in near-field optics [43]. They compare dielectric and topographic contrast [79]. Recently this method was applied to study fluorescence [45] and it was enhanced to calculate near-field above anisotropic samples [36].

12.5 Macroscopic surface integral method

In near-field optical theory Nieto-Vesperinas and A. Madrazo has introduced a generalization of the extinction theorem to multiply connected regions that conducts to an exact calculation of the scattering of any electromagnetic radiation by a cylinder in front of a plane or a relief grating [77, 74]. This calculation is used to model the light emission in STM (Scanning tunneling Electronic Microscope) [73]. It also leads to a 2D global of SNOM, where the tip and the sample are infinite along one direction. The tip is a small cylinder of circular section, the sample is a grating. The formalism take into account the tip sample coupling, determines the far field emission, the field

absorbed by the tip and the near-field structure between tip and sample. By this way Madrazo et al. have studied the detection of surface plasmon [74], the reconstruction of sample surfaces [76]. They apply their formalism to the important problem of the use of near-field optics to data storage [75]. They also envestigate the important theoretical problem of tip-sample coupling; they demonstrate that for a tip diameter smaller than 0.1λ this coupling is very weak.

The extinction theorem is also used in a very interesting discussion of the inverse scattering problem in near-field optical microscopy [37]. A similar method is used in the paper by Maradudin et al. [78]. A 2D model of SNOM is studied with a rather long tapered glass fiber (3λ) in front of a metallic sample.

12.6 First order perturbation method

The methods described above are "rigorous" as they do not suppose any a priori approximation for the calculations. In principle they can be used to study any sample any tip structure and take tip sample coupling into account.

However, they rapidly lead to difficult problems of numerical implementation in a computer. Convergence problems occur very often when the sample (or tip) dimensions become too large. For 3D applications (3D sample and conical tip) they need large memory constraints and the computing time become rapidly extavagant even on a very powerful computer.

Let us notice that the experimental parameters are rarely known with a great precision, and till now an approximative method will be highly appreciated by experimentalists if it leads to a relatively precise estimation of the detected signal in a short time on a small computer.

In near-field microscopy the sample height is generally small compared to the incident wavelength, so a first order perturbation method could be a good approximation to dedermine the electromagnetic fields in a SNOM model.

The first order perturbation method works in Fourier space, it relates the spatial spectrum of the sample roughness to the spatial spectrum of the diffracted field. It leads to simple analytical expressions, that implies very simple and fast algorithms even for 3D sample. Moreover it is easy to discuss the influence of the physical parameters and this method has been firstly used to theoretically describe the principle of STOM [65]. The first papers are in the context of a macroscopic non-global approach, where the sample where a simple 1D grating, but it described the main physical faitures: influence of tip-sample distance on resolution, influence of polarization of the incident beam on image intensity and contrast[7] and it can be used to study the

influence of tip metallization on the images [66].

With the complete formalism (diffraction by a multilayered rough structure [9, 5]), the preliminary studies were enhanced. More complex samples can be studied: 3D samples with overcoating [5, 8]. In that papers, tip-sample is taken into account if necessary which leads to global models of SNOM and STOM

The same formalism can also be used to describe various kinds of tips and study their emission [68, 71, 5]. Recently the perturbation method has also be used to describe the recent experiments of surface plasmon creation and detection by near-field techniques [64].

By introducing the mode structure of an anisotropic medium into the plane wave expansion, the same formalism can be used to described far-field diffraction experiments on magneto-optical samples [70] and to model near-field experiments on such samples [69].

As mentioned above, the perturbation method leads to analytical expressions for the diffracted near-field above the sample surface which considerably simplify the theoretical discussions. R. Carminati and J.J Greffet have thus produced very interessing papers that describe the image formation in near-field microscopy [47], and they have proposed a method of surface profile reconstruction by using near-field data [46].

The images, of a same sample, obtained by the first order perturbation method and the volume integral method are very similar [6].The first order perturbation method seems to be a simple and efficient tool to model scanning near-field optical experiments.

13 Conclusion

This paper is only an introduction to near-field optics and to near-field microscopy and is only a rapid overview of this new domain of Optics. We have explained the principle of near-field microscopy, described the various configurations and rapidly presented the theoretical methods. A study of the bibliography cited in the introduction is necessary to go further in the technical details or to understand theoretical calculations.

Today the development of near-field optical microscopy is very rapid and many applications in many domains are in progress and will be published soon.

The configurations have to be ameliorated in order to obtain more convivial fset-up that can be easily used by a non specialist.

A question is still open, what is the ultimate resolution of near-field optical microscopy. It is not a theoretical limit, but a technological one. By

enhancement of detection, illumination, tip nature and structure the atomic resolution seems a possibility and not a dream.

14 Acknowledgements

I would like to thank, Jean Marie Vigoureux who showed me,15 years ago, the stange and beautiful properties of the evanescent waves. I am deeply grateful to Daniel Courjon who created the Optical Near-field group in my Laboratory and who enables me to participate to this very interesting new field of searches.

References

[1] E. A. Ash and G. Nicholls. Super–resolution aperture scanning microscope. *Nature*, 237:510–52, June 1972.

[2] R. Bachelot, P.H. Gleyzes, and A.C. Boccara. Near–Field optical microscopy by local perturbation of a diffraction spot. *Microsc. Microanal. Microstruct.*, pages 389–397, 1994.

[3] F. Baida, D. Courjon, and G. Tribillon. Combination of a fiber and a silicon nitride tip as a bifunctional detector; first results and perspectives. In D. W. Pohl and D. Courjon, editors, *Near field Optics*, pages 71–78, Netherlands, 1993. Kluwer Academic Publishers.

[4] C. Bainier, S. Leblanc, and D. Courjon. Scanning tunneling optical microscopy: Application to very low relief objects. In D. W. Pohl and D. Courjon, editors, *Near Field Optics*, pages 97–104, Netherlands, 1993. Kluwer Academic Publishers. 114.

[5] D. Barchiesi. A 3-d multilayer model of scattering by nanostructures. application to the optimisation of thin coated nano–sources. *Optics Commun.*, 126:7–13, May 1996.

[6] D. Barchiesi, C. Girard, O.J.F. Martin, D. Van Labeke, and D. Courjon. Computing the optical near–field distributions around complex subwavelength surface structures: A comparative study of different methods. *Phys. Rev. E*, 54(4):4285–4292, October 1996.

[7] D. Barchiesi and D. Van Labeke. Scanning tunneling optical microscopy (STOM): Theoretical study of polarization effects with two models of

tip. In D. W. Pohl and D. Courjon, editors, *Near Field Optics*, volume 242 of *NATO ASI Series*, pages 179–188. Arc et Senans, France, Kluwer Academic Publishers, 1993.

[8] D. Barchiesi and D. Van Labeke. The inverse scanning tunneling near-field microscope (ISTOM) or tunnel scanning near-field optical microscope (TSNOM) 3D simulations and application to nano-sources. *Ultramicroscopy*, 61:17–20, 1995.

[9] D. Barchiesi and D. Van Labeke. A perturbative diffraction theory of a multilayer system, applications to near-field optical microscopy SNOM and STOM. *Ultramicroscopy*, 57:196–203, 1995.

[10] E. Betzig. Principles and applications of near-field scanning optical microscopy (NSOM). In D. W. Pohl and D. Courjon, editors, *Near Field Optics*, volume 242 of *NATO ASI Series*, pages 7–15. Arc et Senans, France, Kluwer Academic Publishers, 1993.

[11] E. Betzig and R. J. Chichester. Single molecules observed by near-field scanning optical microscopy. *Science*, 262:1422–1425, November 1993.

[12] E. Betzig, R. J. Chichester, F. Lanni, and D. L. Taylor. Near-field fluorescence imaging of cytoskeletal actin. *Bioimaging*, 1:129–135, 1993.

[13] E. Betzig, P. L. Finn, and J. S. Weiner. Combined shear force and near-field scanning optical microscopy. *Appl. Phys. Lett.*, 60(20):2484–2486, May 1992.

[14] E. Betzig, M. Isaacson, and A. Lewis. Collection mode near-field optical microscopy. *Appl. Phys. Lett.*, 51(25):2088–2090, December 1987.

[15] E. Betzig, A. Lewis, A. Harootunian, M. Isaacson, and E. Kratschmer. Near-field scanning optical microscopy (NSOM). development and biophysical applications. *Biophys. J.*, 49:269–279, January 1986.

[16] E. Betzig and J. K. Trautman. Near-field optics: microscopy, spectroscopy, and surface modification beyond the diffraction limit. *Science*, 257:189–195, July 1992.

[17] E. Betzig, J. K. Trautman, T. D. Harris, J. S. Weiner, and R. L. Kostelak. Breaking the diffraction barrier: Optical microscopy on a nanometric scale. *Science Reprint Series*, 251:1468–1470, March 1991.

[18] E. Betzig, J.K. Trautman, R. Wolfe, E.M. Gyorgy, P.L. Finn, M.H. Kryder, and C.H. Chang. Near-Field Magneto-Optics and high density data storage. *Appl. Phys. Lett.*, 61:142–144, 1992.

[19] C. Boccara. Voir plus petit. *Pour La Science*, 227:30, 1996.

[20] M. Born and E. Wolf. *Principle of Optics*. Pergamon, New York, 1970.

[21] X. Bouju, C. Girard, and B. Labani. Self-consistent study of the electromagnetic coupling between a thin probe and a surface: implication for atomic-force and near-field microscopy. *Ultramicroscopy*, 1992.

[22] S. K. Buratto, J. W. P. Hsu, E. Betzig, J. K. Trautman, R. B. Bylsma, C. C. Bahr, and M. J. Cardillo. Near-field photoconductivity: Application to carrier transport in ingaasP quantum well lasers. *Appl. Phys. Lett.*, 65(21):2654–2656, November 1994.

[23] D.C Champeney. *Fourier Transforms and their Physical Applications*. Academic Press, London, 1973.

[24] D. Courjon, K. Sarayeddine, and M. Spajer. Scanning tunneling optical microscopy. *Optics Commun.*, 71(1,2):23–28, May 1989.

[25] H.-U. Danzerbink and U. C. Fischer. The concept of an optoelectronic probe for near field microscopy. In D. W. Pohl and D. Courjon, editors, *Near Field Optics*, pages 303–308, Netherlands, 1993. Arc et Senans, France, Kluwer Academic Publishers.

[26] S. Davy, G. Rachard, and M. Spajer. Lithography on PMMA-DR with reflection near field optical microscopy (r-SNOM) and probe characterization. *Proc. Soc. Phot-Opt. Instrum. Eng.*, 2782:551–558, 1996.

[27] F. de Fornel, J.P. Goudonnet, L. Salomon, and E. Lesniewska. An evanescent field optical microscope. *Proc. Soc. Phot-Opt. Instrum. Eng.*, 1139:77–84, 1989.

[28] A. Dereux and D. W. Pohl. The 90° prism edge as a model SNOM probe: Near-field photon tunneling and far-field properties. In D. W. Pohl and D. Courjon, editors, *Near Field Optics*, volume 242 of *NATO ASI Series*, pages 189–198. Arc et Senans, France, Kluwer Academic Publishers, 1993.

[29] R.C. Dunn, E.V. Allen, S.A. Joyce, G.A. Anderson, and X.S. Xie. Near-Field imaging of single proteins. *Ultramicroscopy*, 57:113–117, 1995.

[30] Robert C. Dunn, Gary R. Holtom, Laurens Mets, and X. Sunney Xie. Near-field fluorescence imaging and fluorescence lifetime measurement of light harvesting complexes in intact photosynthetic membranes. *J. Phys. Chem.*, 98(12):3094–3098, 1994.

[31] X.S. Xie AndR.C. Dunn. Probing single molecule dynamics. *Science*, 265:46, 1994.

[32] T.D. Ferrell, S.L. Sharp, and R.J. Warmack. *Ultramicroscopy*, page 408, 1992.

[33] U. C. Fischer. The tetrahedral tip as a probe for scanning near–field optical microscopy. In D. W. Pohl and D. Courjon, editors, *Near Field Optics*, volume 242 of *NATO ASI Series*, pages 255–262. Arc et Senans, France, Kluwer Academic Publishers, 1993.

[34] U. Ch; Fischer and U.T. Dürig D.W. Pohl. Near–Field optical scanning microscopy in reflection. *Appl. Phys. Lett.*, 1988:249–251, 1988.

[35] U.C. Fischer and M. Zapletal. The concept of a coaxial tip as a probe for scanning near field optical microscopy and steps toward a realisation. *Ultramicroscopy*, 42-44:393–398, 1992.

[36] F. Forati, A. Dereux, J.P. Vigneron, Ch. Girard, and F. Scheurer. Theory of kerr effect in magnetic multilayered structures. *Ultramicroscopy*, pages 57–62, 1995.

[37] N. Garcia and M. Nieto-Vesperinas. A direct solution to the inverse scattering problem in Near-Field optical microscopy: Object structure reconstruction. In O. Marti and R. Möller, editors, *Photons and Local Probes*, pages 47–57. NATO ASI Series E 300.

[38] C. Girard. Multipolar propagators near a corrugated surface: implication for local-probe microscopy. *Physical Review B*, 45:1800–1810, 1992.

[39] C. Girard and X. Bouju. Coupled electromagnetic modes bteween a corrugated surface and a thin probe tip. *J.Chem. Phys.*, 95:2056–2064, 1991.

[40] C. Girard and X. Bouju. Self-consistent study of dynamical and polarization effects in near field optical microscopy. *J. Opt. Soc. Am. B*, 9:298–305, 1992.

[41] C. Girard and D. Courjon. Model for scanning tunneling optical microscopy: A microscopic self-consistent approach. *Phys. Rev. B*, 42(15):9340–9349, November 1990.

[42] C. Girard and A. Dereux. Near–field optics theory. *Rep. Prog. Phys.*, 59:657–699, 1996.

[43] C. Girard, A. Dereux, O. J. F. Martin, and M. Devel. Importance of confined fields in near-field optical imaging of subwavelength objects. *Phys. Rev. B*, 50(19):14467–14473, 1994.

[44] C. Girard and M. Spajer. Model for reflection near field optical microscopy. *Applied Optics*, 29(26):3726–3732, September 1990.

[45] Ch. Girard, O. Martin, and A. Dereux. Molecular lifetime changes induced by nanometer scale optical fields. *Phys. Rev. Lett.*, 75:3098–3101, 1995.

[46] Jean-Jacques Greffet, Anne Sentenac, and Rémi Carminati. Surface profile reconstruction using near–field data. *Optics Commun.*, 116:20–24, 1995.

[47] J.J. Greffet and R. Carminati. Theory of imaging in Near-Field microscopy. In M. Nieto-Vesperinas and N. Garcia, editors, *Optics at the Nanometer Scale: Imaging and Storing with Photonic Near Fields*, pages 1–26, Dordrecht, 1996. Nato Asi Series E 200, Kluver Academic.

[48] R. D. Grober, T. D. Harris, J. K. Trautman, E. Betzig, W. Wegscheider, L. Pfeiffer, and K. West. Optical spectroscopy of a gaas/algaas quantum wire structure using near–field scanning optical microscopy. *Appl. Phys. Lett.*, 64(11):1421–1423, March 1994.

[49] Robert D. Grober, Timothy D. Harris, Jay K. Trautman, and E. Betzig. Design and implementation of a low temperature near–field scanning optical microscope. *Rev.Sci.Instrum.*, 65(3):626–631, March 1994.

[50] J. M. Guerra, M. Srinivasarao, and R. S. Stein. Photon tunneling microscopy of polymeric surfaces. *Science*, 262:1395–1400, November 1993.

[51] John M. Guerra. Photon tunneling microscopy. *Appied Optics*, 29(26):3741–3752, September 1990.

[52] B. Hecht, H. Heinzelmann, and D. W. Pohl. Combined aperture SNOM/PSTM : The best of both worlds ? *Ultramicroscopy*, 57(2/3):228–234, 1995.

[53] I. Hörsch, R. Kusche, O. Marti, B. Weigl, and K.J. Ebeling. Spectrally resolved Near-Field imaging of vertical cavity semiconductor lasers. *J. Appl. Phys.*, 79:3831–3834, 1996.

[54] N. Van Hulst, M. Moers, and E. Borgonjen. Applications of Near-Field optical microscopy. In O. Marti and R. Möller, editors, *Photon and Local Probes*, pages 165–187, Dordrecht, 1995. Kluver Academic.

[55] C. Imbert. L'effet inertiel de spin du photon. théorie et preuve expérimentale. *Nouv. Rev. Opt.*, 3:p199, 1972.

[56] C. Imbert and Y. Levy. Déplacement D'un faisceau lumineux par Réflexion totale : Filtrage des états de polarisation et amplification. *Nouv. Rev. Optique*, 6(5):285–296, 1975.

[57] J.D. Jackson. *Classical Electrodynamics*. Number 11. John Wiley. New York, second edition, 1975.

[58] Joshua L. Kann, Tom D. Milster, Fred F. Froehlich, Richard W. Ziolkowski, and Justin B. Judkins. Linear behavior of a near–field optical scanning system. *J. Opt. Soc. Am. A*, 12 No8:1677–1682, August 1995.

[59] Joshua L. Kann, Tom D. Milster, Fred F. Froehlich, Richard W. Ziolkowski, and Justin B. Judkins. Near–field optical detection of asperities in dielectric surfaces. *J. Opt. Soc. Am. A*, 12(3):501–512, March 1995.

[60] F. Keilmann and R. Mertz. Far infrared near field spectroscopy of two dimensional electron system. In D. W. Pohl and D. Courjon, editors, *Near Field Optics*, volume 242 of *NATO ASI Series*, pages 317–324. Arc et Senans, France, Kluwer Academic Publishers, 1993.

[61] Raoul Kopelman, Weihong Tan, Zhong-You Shi, and Duane Birnbaum. Near field optical and exciton imaging, spectroscopy and chemical sensors. In D. W. Pohl and D. Courjon, editors, *Near Field Optics*, volume 242 of *NATO ASI Series*, pages 17–24. Arc et Senans, France, Kluwer Academic Publishers, 1993.

[62] G. Krausch, S. Wegscheider, A. Kirsch, H. Bielefeldt, J. C. Meiners, and J. Mlynek. Near field microscopy and lithography with uncoated fiber tips: a comparison. *Optics Communications*, 119:283–288, 1995.

[63] B. Labani, C. Girard, D. Courjon, and D. Van Labeke. Optical interaction between a dielectric tip and a nanometric lattice: implications for near–field microscopy. *J. Opt. Soc. Am. B*, 7(6):936–942, June 1990.

[64] D. Van Labeke, F. Baïda, and J.M. Vigoureux. *Ultramicroscopy*, page to be published, 1997.

[65] D. Van Labeke and D. Barchiesi. Scanning-tunneling optical microscopy: a theoretical macroscopic approach. *J. Opt. Soc. Am. A*, 9(5):732–738, May 1992.

[66] D. Van Labeke and D. Barchiesi. Probes for scanning tunneling optical microscopy : a theoretical comparison. *J. Opt. Soc. Am. A*, 10(10):2193–2201, October 1993.

[67] D. Van Labeke and D. Barchiesi. Theoretical problems in scanning near–field optical microscopy. In D. W. Pohl and D. Courjon, editors, *Near Field Optics*, volume 242 of *NATO ASI Series*, pages 157–178. Arc et Senans, France, Kluwer Academic Publishers, 1993.

[68] D. Van Labeke, D. Barchiesi, and F. Baida. Optical characterization of nanosources used in scanning near–field optical microscopy. *J. Opt. Soc. Am. A*, 12(4):695–703, April 1995.

[69] D. Van Labeke, A. Vial, and D. Barchiesi. , Near-Field theoretical study of a Magneto-Optical grating. *Ultramicroscopy*, pages 51–55, 1996.

[70] D. Van Labeke, A. Vial, V. A. Novosad, Y. Souche, M. Schlenker, and A. D. Dos Santos. Diffraction of light by a corrugated magnetic grating: experimental results and calculation using a perturbation approximation to the rayleigh method. *Optics Commun.*, 124:519–528, March 1996.

[71] Van Labeke, F. Baida, D. Barchiesi, and D. Courjon. A theoretical model for the inverse scanning tunneling optical microscope (ISTOM). *Optics Commun.*, 114:470–480, 1995.

[72] A. Lewis, M. Issacson, A. Murray, and A. Harootunian. Scanning optical spectral microscopy with 500 a resolution. *Biophys. J.*, 41:405, 1983.

[73] A. Madrazo, Nieto-Vesperinas, and N. Garcia. Exact calculation of maxwell equations for a Tip-Metallic interface configuration: Application to atomic resolution by photon emission. *Phys. Rev. B*, pages 3654–3657, 1996.

[74] A. Madrazo and M. Nieto-Vesperinas. Surface structure and polariton interactions in the scattering of electromagnetic waves from a cylinder in front of a conducting grating: Theory for the reflection photon scanning tunneling microscope. *J. Opt. Soc. Am. A*, 13(4):785–795, 1996.

[75] A. Madrazo and M. Nieto-Vesperinas. Model near field calculations for optical data storage readout. *Appl. Phys. Lett.*, 70(1):31–33, January 1997.

[76] A. Madrazo and M. Nieto-Vesperinas. Reconstruction of corrugated dielectric surfaces with a model of a photon scanning tunneling microscope: influence of the tip on the near field. *J. Opt. Soc. Am. A*, 14(3):618–628, March 1997.

[77] A. Madrazo and M. Nieto Vesperinas. Scattering of electromagnetic waves from a cylinder in front of a conducting plane. *J. Opt. Soc. Am. A*, pages 1298–1309, 1995.

[78] A.A. Maradudin, A. Mendoza-Suarez, E.R. Mendez, and Nieto-Vesperinas. A numerical study of a model Near-Field optical microscope. In M. Nieto-Vesperinas and N. Garcia, editors, *Optics at the Nanometer Scale: Imaging and Storing with Photonic Near Fields*, pages 41–61, Dordrecht, 1996. Nato Asi Series E 200, Kluver Academic.

[79] O. J. F. Martin, C. Girard, and A. Dereux. Dielectric versus topographic contrast in near-field microscopy. *J. Opt. Soc. Am. A*, 13(9):1801–1808, September 1996.

[80] Gail A. Massey, Jeffrey A. Davis, S. M. Katnik, and E. Omon. Subwavelength resolution far-infrared microscopy. *Applied Optics*, 24(10):1498–1501, May 1985.

[81] W. E. Moerner, T. Plakhotnik, T. Irngartinger, U. P. Wild, D. W. Pohl, and B. Hecht. Near-field optical spectroscopy of individual molecules in solids. *Physical Review Letters*, 73(20):2764–2767, November 1994.

[82] M. H. P. Moers, R. G. Tack, O. F. J. Noordman, F. B. Segerink, N. F. Van Hulst, and B. Bölger. Combined photon scanning tunneling microscope and atomic force microscope using silicon nitride probes. In D. W. Pohl and D. Courjon, editors, *Near Field Optics*, volume 242 of *NATO ASI Series*, pages 79–86. Arc et Senans, France, Kluwer Academic Publishers, 1993.

[83] M. NIETO-VESPERINAS. *Scattering and Diffraction in Physical Optics*. J. Wiley, New York, 1991.

[84] L. Novotny, C. Hafner, and D. W. Pohl. The multiple multipole method in near–field optics. In *NFO-3*, volume 8, pages 31–32. Brno, EOS Topical Meeting, 1995.

[85] L. Novotny, D. W. Pohl, and B. Hecht. Light confinement in scanning near field optical microscopy. *Ultramicroscopy*, 61(1-4):1–9, 1995.

[86] L. NOVOTNY, D. W. POHL, and P. REGLI. Light propagation through nanometer-sized structures : The 2-d aperture SNOM. *J. Opt. Soc. Am. A.*, 1993.

[87] Motoichi Ohtsu. Progress of high resolution photon scanning tunneling microscopy due to a nanometric fiber probe. *IEEE Journal of Lightwave Technology*, 13(7):1200–1221, July 1995.

[88] J.D. Pedarnig, M. Specht, and T.W. Hänsch. Fluorescence lifetime variations and local spectroscopy in scanning Near-Field optical microscopy. In O.Marti and R. Möller, editors, *Photon and Local Probes*, pages 151–163, Dordrecht, 1995. Kluver.

[89] A. Piednoir, F. Creuzet, F. Licoppe, and J.M. Ortega. Locally resolved infrared spectroscopy. *Ultramicroscopy*, 57:282–286, 1995.

[90] F. Pincemin, A. Sentenac, and J.J. Greffet. Near-field scattered by sub-surface particles. In D. W. Pohl and D. Courjon, editors, *Near Field Optics*, volume 242 of *NATO ASI Series*, pages 209–220. Arc et Senans, France, Kluwer Academic Publishers, 1993.

[91] D. W. Pohl. Optical near–field scanning microscope. *European Patent Application*, (no0112401), 1982.

[92] D. W. Pohl, W. Denk, and M. Lanz. Optical sthetoscopy:image recording with resolution L/2O. *Appl. Phys. Lett.*, 4:651–653, 1984.

[93] E. Purcell and C.R. Pennypacker. Scattering and absorption of light by nonspherical dielectric grains. *Astro. J.*, 186:705-714, 1973.

[94] R. C. Reddick, R. J. Warmack, and T. L. Ferrell. New form of scanning optical microscopy. *Physical Review B*, 39(1):767–770, January 1989.

[95] V. I. Safarov, V. A. Kosobukin, C. Hermann, G. Lampel, C. Marlière, and J. Peretti. Near-field magneto-optics with polarization sensitive STOM. *Ultramicroscopy*, 57:270–276, 1995.

[96] M. Spajer, D. Courjon, K. Sarayeddine, A. Jalocha, and J.-M. Vigoureux. Microscopie en champ proche par Réflexion. *J. Phys. III*, 1:1, 1991.

[97] M. Specht, J. D. Pedarnig, W. M. Heckl, and T. W. Hänsch. Scanning plasmon near-field microscopy. *Phys. Rev. Lett.*, 68:476–479, 1992.

[98] J. J. Stamnes. *Waves in focal region*. Hilger, Bristol, U.K., 1986.

[99] E. H. Synge. Suggested method for extending microscopic resolution into the ultra-microscopic region. *Philosophical Magazine*, 6:356–362, 1928.

[100] JK Trautman, E. Betzig, JS Weiner, DJ Di Giovanni, TD Harris, F. Hellman, and EM Gyorgy. Image contrast in near–field optics. *J. appl. phys.*, 71:4659–4663, 1992.

[101] G. A. Valaskovic, M. Holton, and G. H. Morrison. Parameter control, characterization, and optimization in the fabrication of optical fiber near–field probes. *Applied Optics*, 34(7):1215–1228, March 1995.

[102] J.M. Vigoueux and D. Courjon. Detection of non radiative fields in light of the heisenberg uncertainty principle and the rayleigh criterion. *Appl. Opt.*, 31:3170–3177, 1992.

[103] H.K. Wickramasyngeand C.C Williams. Apertureless near field optical microscope. *US patent*, (409407034), 1990.

[104] F. Zenhausern, Y. Martin, and H. K. Wickramasinghe. Scanning interferometric apertureless microscopy : Optical imaging at 10 angstom resolution. *Science*, 269:1083–1085, August 1995.

[105] S. Zhu, A.W Yu, D. Hawley, and R. Roy. Frustated total internal reflection: A demonstration and review. *Am. J. Phys.*, 54:601–607, 1986.